# 18

# Two-Dimensional Gel Electrophoresis and Mass Spectrometry in Studies of Nanoparticle-Protein Interactions

Helen Karlsson, Stefan Ljunggren, Maria Ahrén, Bijar Ghafouri, Kajsa Uvdal, Mats Lindahl and Anders Ljungman
*Linköping University; County Council of Östergötland*
*Sweden*

## 1. Introduction

### 1.1 Nanoparticles

Adverse health effects have been associated with the exposure to particulate matter (PM) ever since the London smog in the winter of 1952. Recent estimates attribute about 12,000 excess deaths to have occurred because of acute and persisting effects of the London smog (Bell & Davis, 2001). Over the years a number of epidemiological studies have shown that PM from combustion sources such as motor vehicles contributes to respiratory and cardiovascular morbidity and mortality (Kreyling et al., 2002, 2006, Wick et al., 2010). Especially so do the ultra-fine particles (UFPs) with a diameter less than 0.1 micrometer. UFPs from combustion engines are capable to translocate over the alveolar–capillary barrier (Rothen-Rutishauser et al., 2007). When nano-sized PM (nanoparticles, NP), which are small enough to enter the blood stream, do so they are likely to interact with plasma proteins and this protein-NP interaction will probably affect the fate of and the effects caused by the NPs in the human body. Herein we present results showing that several proteins indeed are associated to NPs that have *in vitro* been introduced to human blood plasma.

NPs are atoms and molecules defined as particles less than 100 nanometers in at least one dimension (Elsaesser & Howard, 2011). Due to the plethora of NPs being produced in various forms (e.g. spherical, fibers, rods, clusters) or by different processes (e.g. flame-spray synthesis, chemical vapor deposition), defining the characteristics of a NP is not an easy task even when it comes to manufactured NPs and when considering those formed unintentionally during processes such as combustion in motor vehicles it becomes an even harder task. This variation in properties according to the respective composition of NPs is also the basis of the wide range of potential applications, from medicine to consumer products. Due to the unique physicochemical properties of nanomaterials, there are plenty of possibilities for NPs to enter the human body, either deliberately as medicines or unintentionally as environmental contaminants and thus potentially cause adverse human health effects (Elsaesser & Howard, 2011; Stern & McNeil, 2008). Although many characteristics have been highlighted as driving the potential adverse health effects associated with NP exposure, it has been specifically the size and increased surface area of NPs that has been concluded as elucidating any such adverse effects observed (Elsaesser & Howard, 2011; Stern & McNeil, 2008).

UFPs from combustion sources, such as motor vehicles, are capable to promote atherosclerosis, thrombogenesis and other cardiovascular events mainly via the ability to induce inflammatory and protrombotic responses (McAuliffe & Perry 2007). Thus, NP induced effects within the lung has been studied over the past twenty years (Mühlfeld et al., 2008; Rothen-Rutishauser et al., 2007). Indeed, exposure to most forms of NPs will initially be via inhalation, especially when considering occupational exposure, and thus will affect the respiratory system. The respiratory system is by far the main port of entry even though the gut and skin are also possible ways of entry. However, NP localization and fate is not only restricted to their portal of entry. NPs can be distributed to organs distal to their site of exposure, so that potential NP toxicity can occur in any secondary site. Research into the possible secondary toxicity of NPs is quite limited. Even so studies investigating the effects of NP translocation to secondary organs have shown that NPs can elicit negative effects to the liver, brain, GI tract (following inhalation), spleen, reproductive systems and the placenta (Kreyling et al., 2002, 2006; McAuliffe & Perry 2007; Wick et al., 2010). NPs toxic mechanisms at the cellular level includes protein misfolding and protein fibrillation causing major problems in the brain and chronic inflammation as a result of nanoparticle exposure, for example in the lung and other organs, via frustrated phagocytosis or production of reactive oxygen species. A vulnerable target for possible toxicological effects of nanoparticles is the fetus. Gold nanoparticles have been shown to cross the maternal-fetal barrier and fullerenes were found to have a fatal effect on mouse embryos (Elsaesser & Howard, 2011; Stern & McNeil, 2008).

When nanoparticles enter the blood vessels, or any biological fluid, e.g. saliva or mucus they are most likely surrounded by a layer of proteins. This dynamic protein "corona" depends on the concentration in the biological fluid and hence the composition of the layer varies in different parts of the body (Cedervall et al., 2007; Lundqvist et al., 2008; Lynch et al., 2007; Walczyk et al., 2010,). Thus, the reactions in the body to such a NP-protein complex is most likely different from that induced by the bare NP and possibly affecting bio-distribution and thereby causing unwanted side effects (Adiseshaiah et al., 2010; Leszczynski 2010,). The function of protein coating is not fully known but since most nanoparticles show strong affinity for proteins, it is of importance to investigate this interaction in different fluids. In blood, plasma proteins constituting the NP corona is possibly affecting a wide range of effects such as phagocytosis via immunoglobulins and complement (Dobrovolskaia & McNeil 2007), coagulation via prothrombin (Dobrovolskaia 2009) and the distribution of lipoproteins (Benderly et al., 2009; Hellstrand et al., 2009; Zensi et al., 2010).

The availability and toxicity of any substance to a biological organism is determined by both the concentration/dose that the organism is exposed to, as well as the "toxicokinetics" of the substance. These include the uptake, transport, metabolism and sequestration to different compartments by the organism, as well as the elimination of the substance from the biological organism. These parameters are essential since the potential toxicity of substances is dependent upon the specific organs or cell types exposed, which form the substance is in (e.g. bound to serum protein, aggregated, dissolved, oxidized), as well as the period of time the substance interacts/remains at the site of primary and secondary exposure. These parameters are influenced by the physical–chemical characteristics of the substance, therefore a detailed characterization of the substance is pivotal in order to allow

generalizable conclusions and should therefore be given ample attention. Furthermore, most of these toxicological parameters involve proteins and/or actions carried out by proteins. Thus it is pivotal to the understanding of NP toxicology, and thereby the possibility to predict health effects caused by NPs, to understand NPs interactions with proteins. One of the best, if not the best, technique to separate proteins is two-dimensional gel electrophoresis (2-DE). Preferably, this is combined with peptide mass fingerprinting and MALDI-TOF MS analyses for fast identification of the separated proteins, which then may be followed by tandem MS analyses for sequence information. Here we present our results regarding serum protein interactions with metal-nanoparticles ($Al_2O_3$, ZnO/Al6%, $SiO_2$) and Carbon Nanotubes, obtained using 2-DE and MS. Furthermore, we elaborate on and exemplify different aspects of the 2-DE/peptide mass fingerprinting-technique to further improve the approach.

### 1.2 General introduction to the 2-DE technique

Two-dimensional gel electrophoresis (2-DE) is an excellent method for separation of proteins from most kinds of tissues and complex mixtures of proteins (O`Farrel-1975). Both qualitative characterization of the protein expression, including post-translational modifications and quantitative characterization comparing the protein expression in different individuals or groups, are possible by this technique. Two steps are included, the isoelectric focusing (IEF) step, where the proteins are separated according to their isoelectric point (pI) in a pH-gradient, and the sodium dodecyl sulphate polyacrylamide gel electrophoresis (SDS-PAGE) step, where the proteins are separated according to their molecular weight. Since it is less common that two proteins have the same isoelectric point and molecular weight, this will result in each protein migrating to its own unique position. The 2-DE technique allows, depending on the nature of the sample, the separation of 500-3000 protein spots and the resolution can be improved, e.g. by removal of abundant proteins or by composite gels from overlapping pH-gradients. Proteins separated by gel electrophoresis can be visualized by a number of methods using different types of stains. Various stains interact differently with the proteins and some of the stains used are not even specific for proteins. The degree of sensitivity is also different. Processing data from stained protein gels by computers includes the gel images being digitized by an imaging system and then analyzed using computer software allowing a number of different measurements such as number, size, and intensity of the stained protein spots. Separated proteins are then identified by mass spectrometry (MS). The proteins are in-gel digested and extracted peptides analyzed by peptide mass fingerprinting or peptide sequencing. Two widely used MS instruments used for these respective analyses are matrix assisted laser desorption/ionization-time of flight-mass spectrometry (MALDI-TOF MS) where peptides are transferred from solid phase to gas phase, and electrospray ionization tandem mass spectrometry (ESI MS/MS) where peptides are transferred from liquid phase to gas phase. The key advantage with 2-DE is the ability to separate protein isoforms. On the other hand, very large and hydrophobic proteins are underrepresented in 2-DE and the need of peptide extraction from the in-gel digests may influence to amounts of analytes available for MS protein identification. Nevertheless, combining the separation and analytical ability of the 2-DE technique with the identification power of MS provides a powerful tool in human toxicology.

## 2. Methods

### 2.1 Characterization of nanoparticles

Commercial $SiO_{2\ size\ 0.007\mu}$ (S-3051), ZnO/6% Al doped $_{<50nm}$(677450), and $Al_2O_{3\ <50nm}$ (544833) were purchased from Sigma Aldrich. As comparison, single walled Carbon Nanotubes (CNO, 704121) from Sigma Aldrich was used. Nanoparticles, characterized by manufacturer, were dispersed in Milli-Q water and/or PBS (137 mM NaCl, 2.7 mM KCl, 8.45 mM $Na_2HPO_4$, 1.47 mM $KH_2PO_4$ pH 7.3) and sonicated on ice for 10 min. The hydrodynamic sizes of the particles were analyzed by Dynamic Light Scattering (DLS).

DLS measurements were performed using an ALV/DLS/SLS-5022F system (ALV-GmbH, Langen Germany) and a HeNe laser at 632.8 nm with 22 mW output power. The scattering angle was 90° and the temperature 22°C. For temperature stabilizing purposes, samples were placed in a thermostat bath (22°C) for at least 10 minutes prior to the measurements. Samples were diluted in Milli-Q water or PBS. Ultrasonication of two different kinds was performed to decrease the degree of agglomeration; either an ultrasonic bar homogeniser (Sonoplus HD 2200, Bandelin electronics, Germany) was used or samples were placed in an ultrasonic bath (USC300T, VWR, Sweden). The viscosity of PBS was set to 0.9782 mPa's by linear interpolation between tabulated values for 20°C (0.911) and 25 °C (1.023) (Hackley & Clogston, 2007).

Data analysis was performed using a nonlinear fit model via ALV-Regularized Fit (ALV-Correlator Software Version 3.0. using ALV-Regularized in nonlinear fit model http://www.alvgmbh.de/).

### 2.2 Preparation of human plasma

Human plasma, collected in sodium citrate tubes, was prepared from three healthy volunteers. After cooling, the blood was centrifuged in 800g for 10 min and plasma, free from red blood cells, was drawn from the top of the tube. $SiO_2$, ZnO/6% Al doped, $Al_2O_3$ and CNO were then exposed to three plasma samples respectively. In all nanoparticle exposures fresh plasma was used.

### 2.3 Nanoparticle/plasma incubation

Nanoparticles were dissolved (final concentration 2 mg/ml) in PBS and incubated with 1% plasma at 37˚C for 1h. As control, to ensure there was no protein precipitation, one sample was prepared without nanoparticles. Unbound proteins were separated from nanoparticles by centrifugation for 40 min at 50 000g and 4°C. The supernatant was discarded and the particle pellet was washed in Dithiothreitol (DTT, Sigma-Aldrich) 20mM/-acetone buffer followed by a second centrifugation step for 10 min at 50 000g and 4°C. The supernatant was discarded and the pellet was air dried. The pellets containing nanoparticles and attached proteins were then dissolved in denaturing solution containing 9M Urea (Sigma-Aldrich), 65mM DTT and 4% (3-(3-cholamidopropyl)-dimethylamino)-1-propanesulfonate (CHAPS). The solution was incubated at room temperature for 30 min before denatured proteins were separated from the nanoparticles by centrifugation for 30 min at 50 000g and 4°C. The supernatant was collected and the samples were analyzed in triplicates. 20 µl (40µg protein) was applied on the IEF strip in each 2-DE analysis.

### 2.4 Isolation of lipoproteins

#### 2.4.1 HDL isolation

Preparation of high density lipoprotein (HDL) was performed by a method described by Sattler et al.1994, with slight modifications (Karlsson et al., 2005). Blood samples in EDTA-containing tubes were obtained from healthy volunteers after an overnight fast. After centrifugation (10 min, 700*g*) at room temperature, plasma was collected. EDTA (1 mg/mL) and sucrose (final concentration 0.5%) were added to prevent HDL oxidation and aggregation, respectively. Five milliliters of EDTA-plasma adjusted to a density of 1.24 g/mL with solid KBr (0.3816 g/mL) was layered in the bottom of a centrifuge tube (Beckman, Ultraclear tube). The EDTA plasma fraction was gently overlayered with KBr/PBS solution (0.0834 g KBr/mL, total density 1.063 g/mL). In one centrifuge tube, proteins were stained with Coomassie Brilliant Blue to be used as a reference while collecting the HDL fraction. Ultracentrifugation was performed in a Beckman XL-90 equipped with a Ti 70 rotor (fixed angle; Beckman Instruments, Fullerton, CA, USA) for 4 h at 290 000*g* and 15°C. By this procedure the lipoprotein fractions with a density lower than 1.063 g/mL (low density and very low density lipoprotein) are located at the top of the tube and HDL is located in the middle of the tube. HDL was collected by penetrating the tube with a syringe. To avoid contamination by serum proteins, HDL were then further purified by a second centrifugation step. KBr/PBS solution (0.3816 g KBr/mL) was added to the HDL (total density 1.24 g/mL) and the centrifugation was performed under the same conditions as described above, but for 2 h. HDL was collected from the top of the tube and desalted using desalting buffer ($NH_4HCO_3$, 12mM, pH 7.1) and PD 10 columns (Sephadex™ G-25 M, GE Healthcare, Buckinghamshire, United Kingdom ). Protein concentration in the HDL solution was determined with Bio-Rad protein assay (Bio-Rad, Richmond, CA, USA). Sample (3.5 mL) was lyophilized and dissolved in 0.25 mL sample solution (9 M Urea, 4% CHAPS, 2% Pharmalyte , 65 mM DTT, 1% bromophenol blue) according to Görg et al.1988.

#### 2.4.2 Immunoaffinity chromatography

Anti-ApoA-I antibodies were attached to a 5 mL HiTrap NHS-activated HP column (GE Healthcare) according to manufacturer's instructions. 2.5 mL plasma were desalted by the use of PD-10 columns and the eluted sample were diluted to 4 mL with 50 mM Tris-HCl, 0.15M NaCl, pH 7.5. The ApoA-I coupled immunoaffinity column were equilibrated by allowing 10 column volumes flow through it. Desalted sample were applied into the column and allowed to recirculate for 40 minutes. Loop were disconnected and washed with 10 column volumes of 50 mM Tris-HCl, 0.15M NaCl, pH 7.5 followed by ten column volumes of 50 mM Tris-HCl, 0.5M NaCl, pH 7.5. ApoA-I adsorbed to the column were eluted with 20 mL of 0.1M Glycin-HCl, pH 2.2. Sample was collected in fractions of 0.4 mL in tubes which each contained 20 µL 1M Tris, pH 9.0 for pH-neutralization of the sample. Fractions containing proteins were pooled and desalted using PD-10 columns.

### 2.5 Albumin and IgG removal

The removal of the high abundance proteins albumin and IgG from plasma was performed using an Albumin and IgG removal kit (GE Healthcare). Briefly, the column was equilibrated with binding buffer (20mM $Na_2H_2PO_4$, 0.15M NaCl, pH 7.4), 50 µl of plasma

was diluted to a volume of 100 µl and applied to the column. After 5 min incubation, the depleted sample was collected in an eppendorf tube by centrifugation at 784g. The total protein concentration before/after depletion was determined with Bio-Rad protein assay. After depletion of high abundant proteins the samples were desalted using PD-10 columns.

### 2.6 2-DE analysis

2-DE was performed using IPGphor and Multiphor (GE healthcare). Briefly, the proteins were resuspended in 150 µL of a 2-DE sample buffer containing 9 M urea, 65 mM DTT, 2% Pharmalyte (GE Healthcare), 4% CHAPS, and 1% bromophenol blue and then centrifuged at 4ºC and 23000g for 30 min to remove debris. The supernatant was then mixed with a rehydration buffer consisting of 8 M urea, 4% CHAPS, 0.5% IPG buffer 3-10 NL (GE Healthcare), 19 mM DTT, and 5.5 mM Orange G to a final volume of 350 µL. The first dimension was performed by in-gel rehydration for 12 h in 30 V on 18 cm pH 4-7 linear or pH 3-10 nonlinear IPG strips (Immobiline DryStrips, GE Healthcare). The proteins were then focused at 53000 Vh at a maximum voltage of 8000 V (Görg et al., 2000). The second dimension (SDS-PAGE) was performed by transferring the pI focused proteins (IPG strips) to homogeneous or gradient home-cast gels on gel bonds. The electrophoresis was performed at 40-800 V, 10°C, 20-40 mA, overnight.

### 2.7 Staining and image analysis

Sypro Ruby (Bio-Rad) staining were done according to manufacturer's instructions. In short, gels to be stained with Sypro Ruby were directly placed in a fixing solution containing 10% methanol and 7% acetic acid for at least 20 minutes after 2-DE. Gels were then washed 3x10 minutes under agitation with Milli-Q water before approximately 400 mL of Sypro Ruby stain were added and incubated in room temperature over night.

Silver staining of gels were done according to Shevchenko et al. 1996, with some few modifications. Proteins were fixed by incubating the gel in 50% methanol and 5% acetic acid for at least 20 minutes directly after 2-DE and then incubated with 50 % Methanol for 5 minutes, followed by Milli-Q water for 10 minutes. In the sensitizing step the gel was incubated with 0.02 % sodium thiosulphate for 1 minute, followed by 2x1 minutes washing with Milli-Q water. The gel was then immersed in 0.1 % silver nitrate solution for 20 minutes before excess of silver was washed away by 2x1 minute in Milli-Q water. Next, the gel was developed in 0.04 % formaldehyde in 2 % sodium bicarbonate solution for 2x1 minute. The exact developing time was optimized depending of the protein amount in the gel. Finally, the reaction was stopped by incubation 1x5 min in 0.5 % glycine and the gel washed with Milli-Q water for 2x20 min.

The images of the protein patterns were analyzed by a CCD (Charge-Coupled Device) camera digitizing at 1340*1040 pixel resolution in a UV scanning illumination mode for Sypro Ruby stained gels or at 1024*1024 pixel resolution in white light mode for silver stained gels using a Flour-S-Multi Imager in combination with a computerized imaging 12-bit system (PDQuest 2-D gel analysis software, version 7.1.1). The unit of the UV light source is expressed in counts while the unit of the white light source is expressed as optical density (OD). Gel images were evaluated by spot detection, spot intensities and geometric properties.

### 2.8 Isolation of protein spots

Protein spots were excised from the gels using a syringe and transferred to eppendorf tubes. For silver destaining, 25 µL of 100 mM sodium thiosulphate and 25 µL of potassium ferricyanide were added to the gel pieces (Gharahdaghi et al., 1999). When the pieces were completely destained, the chemicals were removed by washing (6×5 min with Milli-Q water) before addition of 50 µL of 200 mM ammonium bicarbonate and incubation for 20 min at room temperature. The gel pieces were washed (3x5 min with Milli-Q water) and dehydrated with 100% acetonitrile (ACN) for 5 min or until the gel pieces were opaque white. After removal of the ACN, the gel pieces were dried in a SpeedVac vacuum concentration system (Savant, Farmingdale, NY). Protein spots excised from Sypro Ruby stained gels were washed in 50% ACN/25 mM ammonium bicarbonate 2x30 min prior to dehydration with 100% ACN.

### 2.9 Digestion

#### 2.9.1 Tryptic digestion

The protein spots were excised from the gel with a syringe and transferred to small eppendorf tubes (0.5 mL). Proteins from fluorescently stained gels were visualized and excised on a blue light transluminator (DR-180 B from Clara Chemical Research, Denver, CO, USA) wearing darkened amber glasses. After destaining and dehydration, about 25 µL trypsin (20 mg/mL in 25 mM ammonium bicarbonate, Promega, Madison, WI, USA) was added to each gel piece. To minimize autocatalytic activity, the samples were kept on ice for 30 min, prior to incubation in 37° C over night. The supernatant was transferred to a separate tube and the peptides were further extracted from the gel piece by incubation in 50% ACN/5% trifluoroacetic acid (TFA, Sigma-Aldrich) for 5 h at room temperature. The supernatant from the two steps was then pooled and dried in SpeedVac until complete dryness. If not dissolved in 5 µL 0.1% TFA for further MS preparation, the proteins were stored at -70°C.

#### 2.9.2 Glu-C digestion

Glu-C (Roche, Basel, Switzerland) was diluted with 25 mM $NH_4HCO_3$, pH 7.8, to a concentration of 20 µg/mL. 25 µL was added to each gel piece and incubated at room temperature over night. The supernatant was then dried in SpeedVac until complete dryness. If not dissolved in 5 µL 0.1% TFA for further MS preparation the proteins were stored at -70°C.

#### 2.9.3 Cyanobromide digestion

One Cynobromide (CNBr, Sigma-Aldrich) crystal was dissolved in 250 µL 70% TFA (in $dH_2O$). 25 µL CNBr in 70% TFA was added to the dried gel piece and incubated in darkness in room temperature overnight. The supernatant was then dried in SpeedVac until complete dryness. If not dissolved in 5 µL 0.1% TFA for further MS preparation the proteins were stored at -70°C.

#### 2.9.4 Endoproteinase Asp-N digestion

Asp-N (P3303, Sigma-Aldrich) was diluted with 100 mM $NH_4HCO_3$ pH 8.5 to an enzyme concentration of 8 µg/mL. 25 µL was added to one tube containing one gel piece. To minimize autocatalytic activity, the samples were kept on ice for 30 min, prior to incubation

in 37° C over night. The supernatant was then dried in SpeedVac until complete dryness. If not dissolved in 5 µL 0.1% TFA for further MS preparation the proteins were stored at -70°C.

### 2.9.5 Enzymatic deglycosylation

HDL (500 µg) was lyophilized and dissolved in 100 µL 2-DE sample buffer (described earlier).The sample was then incubated with 20 U of PNGase F (Sigma-Aldrich, P7367) in 37˚ C over night. After incubation, sample were stored in -20°C until 2-DE.

HDL was desalted in a PD-10 column and eluted in a 50 mM $Na_2HPO_4$, pH 6.0 buffer. A volume corresponding to 1200 µg of HDL proteins were then incubated with 10 U of Neuraminidase (Sigma-Aldrich, N3786) in 37˚ C for 4 hours. After incubation, sample was desalted in a PD-10 column with desalting buffer ($NH_4HCO_3$, 12mM, pH 7.1) and subsequently frozen in -70°C. Sample was lyophilized before 2-DE.

### 2.10 ZipTip

After digestion and drying of peptide samples, some were desalted and purified by the use of $ZipTip_{C18}$® pipette tips (Millipore, Billerica, MA, USA). Samples were diluted up to 10 µL with 0.1% TFA. A ZipTip was wet by loading 3x10 µL with 50% ACN and discarding the liquid. Ziptip was equilibrated by loading 3x10 µL of 0.1% TFA and discarding the fluid before peptide sample was carefully loaded into the ZipTip by pipetting. The ZipTip was washed with 5x10 µL of 0.1% TFA before peptides were eluted with 10 µL 50% ACN.

### 2.11 Mass spectrometry

Peptides obtained after digestion were mixed 1:1 with matrix, α-Cyano-4-hydroxycinnamic acid (CHCA, 0.02 mg/mL) or 2,5-dihydroxybenzoic acid (DHB, 0.02 mg/mL) in 70% ACN/0.3% TFA, and then spotted onto a stainless steel target plate. Analyses of peptide masses were performed using MALDI TOF-MS (Voyager DE PRO; Applied Biosystems) equipped with a 337 nm N2 laser operated in reflector mode with delayed extraction. Positive ionization, a delay time of 200 ns, and an accelerating voltage of 20 kV were used to collect spectra in the mass range of 600–3600 Da. Data processing of the spectra was performed in a Data Explorer TM Version 4.0 (Applied Biosystems). External mass calibration with a standard peptide mixture and internal calibration using known trypsin autolysis peaks (*m/z* 842.5100, 1045.5642, 2211.1046) were also performed prior to the database search. For tandem MS analysis, the digested peptides were dried and dissolved in 10 µL 0.1% TFA. The peptides were desalted and purified by using $ZipTip_{C18}$® columns. Elution was acidified by the addition of 1% formic acid. About 2 µL of the sample was applied into a silver-coated glass capillary and analyzed by a hybrid (triple quadrupole-TOF) mass spectrometer (API Q-STAR Pulzer; Applied Biosystems) equipped with a nanoelectrospray ion source (MDS-Protana, Odense, Danmark) operated in the nanopositive mode. Data processing was performed with Analyst QS software (Applied Biosystems). Fragmentation spectra were interpreted manually.

### 2.12 Database search

Peptide masses (major peaks) in the spectra were submitted to database search. NCBI and Swiss-Prot were used with Aldente or MS-Fit as search engines. Restrictions were human

species, mass tolerance >75 ppm in most of the searches, maximum one missed cleavage, and cysteine modification by carbamidomethylation. MS-Digest, MS product, and BLAST search was used for protein identification of the derived tags resulting from amino acid sequencing with MS/MS. In peptide mass fingerprinting, protein matches with p-values below 0.05 are used and with LC-MS/MS analyses an FDR $\leq$ 1 % is considered significant.

### 2.13 Western blot

Plasma proteins were separated on 2-DE. Proteins were then transferred to a 0.2 µm PVDF membrane. After blocking with 5% non-fat dry milk in Tris buffered saline (TBS) overnight, the membrane was washed two times with Tween-Tris buffered saline (TTBS, pH 7.5) and then incubated overnight with primary rabbit anti human C-III antibodies (Abcam, 21032, 1:5000) in 2% non-fat dry milk in TTBS (pH 7.5) at room temperature. After washing four times with TTBS, the membrane was further incubated for 1h with secondary goat anti rabbit antibodies conjugated with horse radish peroxidase (HRP, 170-6515, BioRad,1:40 000) in 2% non-fat dry milk in TTBS (pH 7.5) at room temperature. In order to visualize the proteins the PVDF membrane was treated with ECL Plus Western Blotting Detection System (GE Healthcare) and then exposed to X-ray film (AGFA Medical, Mortsel, Belgium).

## 3. Results and discussion

### 3.1 Nanoparticle characterization

DLS, which is also known as Photon Correlation Spectroscopy or Quasi-Electron Light Scattering, is a technique used to study the size and size distribution of particles suspended in a liquid. The technique is based on the scattering of light of particles in diffusive random (brownian) motion. The average displacement for the Brownian motion is defined by the translational diffusion coefficient (D). The particle diffusive motion in liquid is size dependent, and a larger particle has a slower motion as compared to a smaller particle. This brownian motion can be investigated by irradiating the sample with a coherent laser and studying the intensity fluctuations of the scattered light (Finsy, 1994).

Particle sizing can be done in several ways. Typically the information retrieved from different techniques is to some extent diverse, as each technique is sensitive to it´s specific properties of the particles. That means that a technique which is based upon the scattering intensity does not deliver the same size or size distribution as a technique that is based upon the projected area or the density of a nanoparticle. For nano sized particles, transmission electron microscopy (TEM) is frequently used in purpose to study the size and the shape of particles. In TEM, the sample preparation together with the measurement is relatively time consuming and furthermore the measurement is limited only to a very small fraction of the sample. This means that a lot of replicates must be studied in order to achieve good statistics. A dynamic light scattering measurement on the other hand, is fast and convenient as it usually takes only a few minutes to perform. Data recording procedure is thus short but the analysis and interpretation requires knowledge and care. DLS measurements must be performed with highly diluted solutions, to avoid multiple scattering phenomenons and misleading artifacts are frequently present in DLS studies.

Particle sizes obtained when measuring with DLS are by default larger than those obtained when analyzing the material with TEM. The size calculated from the translational diffusion

coefficient in DLS generally is referred to as the hydrodynamic diameter, e.g the diameter of a sphere having the same diffusion coefficient as the particle, while the size of the nanoparticles obtained from TEM is the core size of the nanoparticle investigated. It should be noted that in many cases when the sample consists of a mixture of nanoparticles with a range of sizes and/or mixture of particle shapes, results should be taken as an estimation only but clearly trends can be observed.

The autocorrelation function of the scattered intensity results in an average value of the product of the intensity at time t and the intensity at a time delay later t+dt. The value obtained from the correlation function is large for short delays, since the intensities are highly correlated. The value will be low for longer delays; i.e. the autocorrelation can be described as a decaying function of time delay. From the autocorrelation function, the diffusion constant D can be determined. Furthermore, by using Stokes-Einstein equation the corresponding size distribution is calculated according to:

$$d = k_B T / 3\pi\eta D \quad (1)$$

where $k_B$ is the Boltzman constant, T the temperature, η the viscosity of the solvent and d the hydrodynamic diameter of the particles. This implies that the temperature must be constant during the measurement and the viscosity of the sample solvent must be known. It should be noted that the formula shown above (Equation 1) is valid only for non-interacting spherically shaped particles, i.e experimental data are fitted to a model assuming spherical particles (Finsy, 1994).

Figure 1 shows five different functions representing the typical information retrieved in DLS in the actual measurement and by using algorithms. The measured data in DLS is the correlation function (Figure 1A). This function holds information about the diffusion of particles in the sample and can be transformed to a graph showing the decay time of light scattering fluctuations (Figure 1B). From the decay time distribution function, the values of the particle radius (Figure 1C) can be calculated using the Stokes-Einstein equation.

The amount of light that is scattered from a particle is dependent on the particle size. According to the Rayleigh theory (Sorensen, 2008), the scattering factor roughly is proportional to the sixth power of the particle size. This means that a small particle scatter light less than a larger particle and thus different weights have to be applied to transform the intensity weighted data to a useful size distribution. These weights can be mass based (Figure 1D) or number based (Figure 1E). Powder based samples that are dispersed in a liquid often are severely aggregated. Ultrasonic baths can be used to decrease the aggregation in the solution. Choice of solvent is also important and it clearly affects the capability of dispersing nanoparticles.

A number of examples of DLS results for commercial particles are shown in Figure 2, 3 and 4. The size distributions of $Al_2O_3$ nanoparticles , based upon number weighted fits of the data are shown in Figure 2. A set of samples were dispersed both in Milli-Q water and PBS. The size and size distribution were measured as a function of concentration. According to the supplier these particles are < 50 nm in size as measured by TEM, which should be taken as the core size of the nanocrystals in the $Al_2O_3$ material. A lot larger hydrodynamic diameters are achieved in our measurements, which show that the water based sample is

composed of at least two populations with hydrodynamic radius of about 100 nm and 200-300 nm respectively. The smallest radius from this DLS study was achieved for $Al_2O_3$ dispersed in Milli-Q water and ultrasonicated with a bar homogenizer (radius approx. 30 nm). Also for samples dispersed in PBS, ultrasonication with a bar homogenizer indicates decrease of the aggregation and introduction of populations with smaller radius.

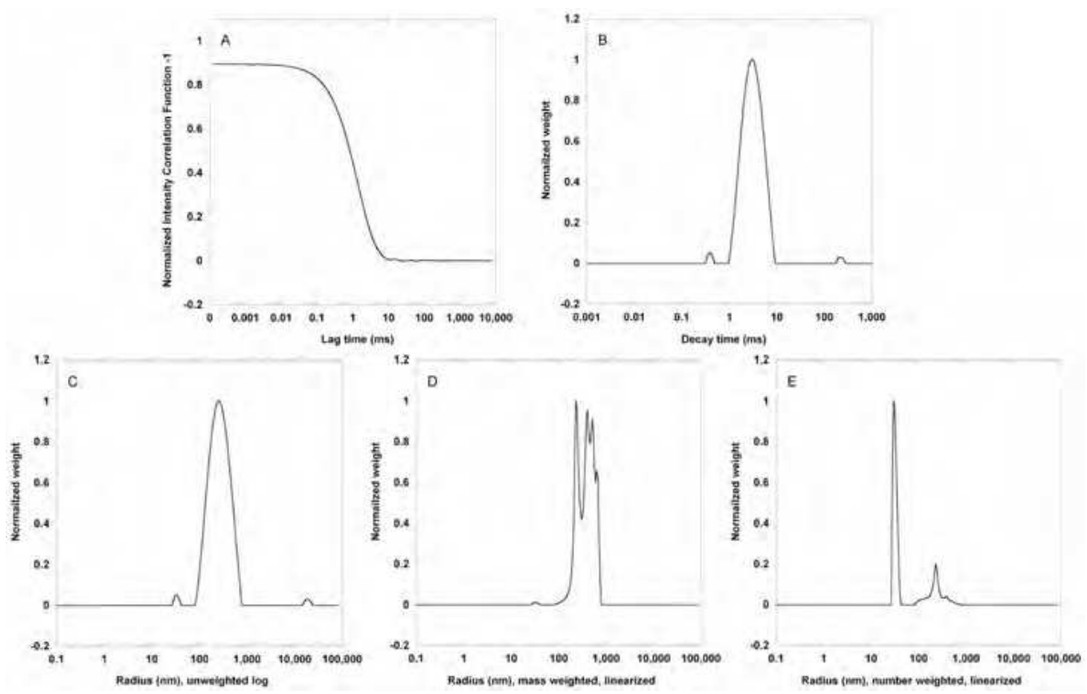


Fig. 1. Example of the typical information retrieved in a DLS measurement.
The measurement is performed on Al doped ZnO nanoparticles dissolved in MilliQ water. A) shows the correlation function which has a high correlation (close to 1) for really short lag times but decays to zero with a rate dependent on the particle size distribution in the sample. B) shows the normalized distribution function of the Decay time. C) shows the normalized distribution of the unweighted radius and the corresponding normalized distributions of the mass weighted radius and the number weighted radius are shown in D) and E) respectively.

Figure 3 shows the size distribution of Aluminium doped ZnO nanoparticles dispersed in water and PBS. Bar ultrasonication introduces smaller sized populations, in consistence with the results in Figure 2. The hydrodynamic radii of these particles in MilliQ water are around 30 nm as largest according to Figure 3. This could be compared with the information from the supplier that these particles are < 50 nm as measured by TEM. Again hydrodynamic diameter is always larger that the core size of nanocrystals obtained from TEM. In this case the sample is also aggregated in solution, which produces even larger sizes and size distributions.

The $SiO_2$ particles are 7 nm sized as primary particles according to the supplier based on calculations using the surface area as measured by the nitrogen adsorption method of Brunauer (Brunauer et al., 1938). The supplier also states that these particles commonly form

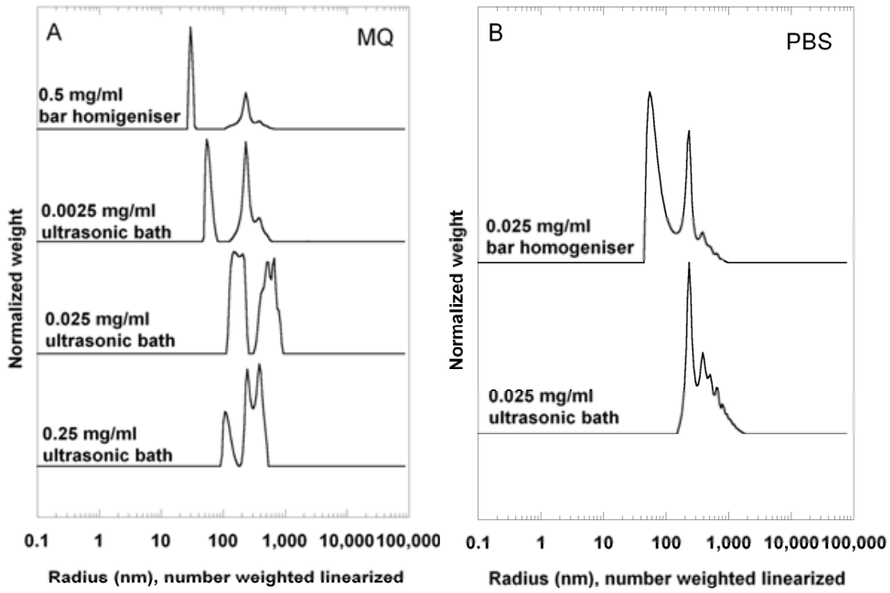


Fig. 2. DLS measurements of $Al_2O_3$ nanoparticles.
The normalized distribution of the number weighted radii of particles in $Al_2O_3$ nanopowder diluted to different concentrations in A) MilliQ and B) PBS as measured by DLS. As marked in the figure, two different kinds of ultrasonic treatment were used to decrease the aggregation before performing the measurement; either an ultrasonic bath or a bar homogenizer.

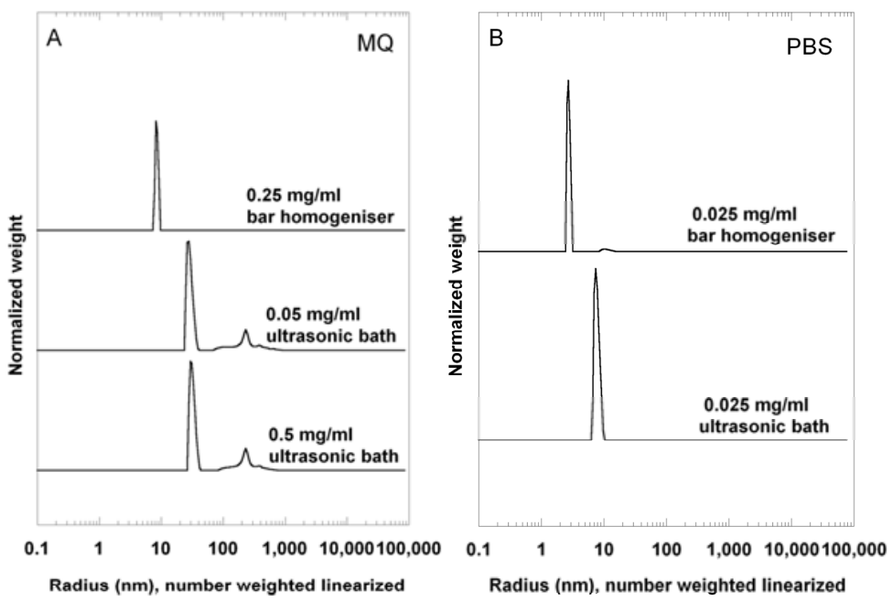


Fig. 3. DLS measurements of ZnO (Aluminium 6% doped) nanoparticles.
The normalized distribution of the number weighted radii of particles in ZnO (Aluminium 6% doped) nanopowder diluted to different concentrations in A) MilliQ and B) PBS as measured by DLS. As marked in the figure, two different kinds of ultrasonic treatment were used to decrease the aggregation before performing the measurement; either an ultrasonic bath or a bar homogenizer.

some hundreds of nanometer long chainlike branched aggregates. The size distributions obtained in our DLS measurements are presented in Figure 4. For all three concentrations in Milli-Q water the particle size is below 100 nm in radius. When $SiO_2$ particles are dispersed in PBS (Figure 4B), large aggregates are definitely present, which are partly removed when ultrasonicated with a bar homogenizer. Multiple scattering, surface charge on the nanoparticles and water solubility should be considered when further evaluating these data. Furthermore, it is known that these specific samples ($SiO_2$) are inhomogenous and the sample is thus far from ideal, i.e does not contain spherical shaped particles. It is shown in previous studies that long chainlike branched aggregates are present.

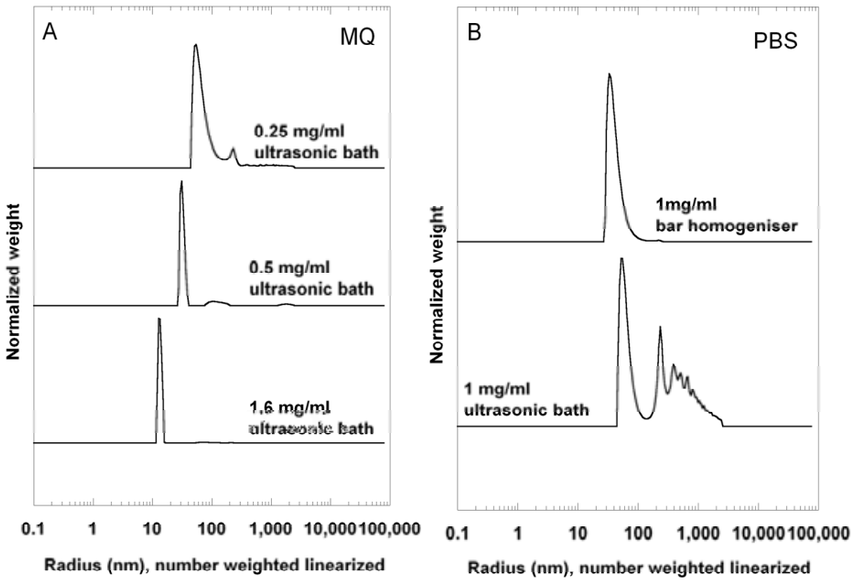


Fig. 4. DLS measurements of $SiO_2$ nanoparticles.
The normalized distribution of the number weighted radii of particles in $SiO_2$ nanopowder diluted to different concentrations in A) MilliQ and B) PBS as measured by DLS. As marked in the figure, two different kinds of ultrasonic treatment were used to decrease the aggregation before performing the measurement; either an ultrasonic bath or a bar homogenizer.

In conclusion, it could be said that size and size distribution of nanoparticle samples could be estimated by DLS. Valuable information as the trends in size distribution connected to sample preparation methods and choice of solvent can be obtained. Sample preparation methods are indeed very important as well as choice of solvent. Care should be taken when choosing fitting model and the model-inbuilt parameters. Inhomogeneous samples are less straight forward to analyze. Presence of aggregates is easily detected. In summary information obtained from DLS is important for everybody that is doing research on nanoparticles in liquids. The numbers given as product information i.e. the size and size distribution, are often relevant for the core-size of the nanocrystals within the material. However the nanoparticles are most often not soluble to that extent. Nanoparticles obtained in dry state and then dispersed in liquid usually form aggregates as shown in this study.

### 3.2 Nanoparticle-plasmaprotein interactions

In a previous study performed by us, the inflammatory response in human monocyte derived macrophages after exposure to wear particles generated from the interface of studded tires and granite containing pavement (Karlsson et al. 2011) was investigated. Particle characterization showed that dominating peaks in the EDX spectra were Silica and Aluminium. Particles of nanosize were also present (SMPS), but it was not possible to characterize them due to low abundance. As a result of their very small diameter (< 0.1 μm), inhaled nanoparticles are believed to be predominantly agglomerated and deposited in the periphery of the lungs, where they interact with cells such as macrophages and epithelial cells (Beck-Speier et al. 2005) but they may also translocate into the circulation, which is a critical step, since their fate *in vivo* in not known. Investigating plasma protein-nanoparticle interactions with a toxico-proteomic approach is a useful tool to improve our knowledge about the effects of nanoparticles of different origin, size and surface properties in biological systems.

In purpose to mimic a potential exposure to airborn nanoparticles translocated into the circulation, commercial $SiO_2$ and $Al_2O_3$ were mixed with plasma proteins. As comparison, commercial ZnO (Al-doped 6%) and a non-metal oxide; single walled Carbon Nanotubes was used. All preparations were performed in triplicates with three different subjects exposed to each type of particles. The protein patterns resulting from the three different exposures of commercial $SiO_2$, $Al_2O_3$, ZnO and CNO respectively were identical.

Particle characterization and estimation of particle agglomeration prior to exposure is crucial. In a recent study of nanoparticle-plasma protein interactions (Deng et al. 2009), the DLS spectra indicated large agglomerates prior to plasma protein exposure. Most likely, and in line with the authors suggestions (Deng et al. 2009), complexes with hydrodynamic size of 10000-100 000 nm do not result in the same protein patterns as the interactions of smaller particles/agglomerates and plasma proteins. In our optimized protocol, with different particle origin, less gentle bar sonication instead of in water bath and thereby reduced hydro dynamic sizes of the agglomerates (Fig 2-4) - an altered pattern of interacting proteins was indeed found (Figure 5, Table 1).

Interestingly, the interaction of $SiO_2$ and CNO with plasma proteins resulted in very similar protein patterns despite their different properties (Fig 5). It has to be stated though, that the fate of CNO in the lung may not be translocation into the circulation due to the tube like structure, but CNO is also of interest for medical applications (Wu et al. 2011).

The transport proteins Albumin and Alpha-2-HS-glycoprotein interacted with $SiO_2$, CNO and ZnO but not $Al_2O_3$ while Transferrin interacted with $SiO_2$, $Al_2O_3$ and notably also CNO but not ZnO. Supporting our results, the binding of albumin to single walled CNO has previously been described to promote uptake by the scavenger receptor in RAW cells (Dutta et al., 2007). In line, intravenous administration of CNO has in a different study resulted in high localization in the liver (Cherukuri et al., 2006). Another possible way for nanoparticles into the cells, are as Transferrin/particle complexes that are able to enter the cells via the Transferrin receptor. The Transferrin receptor is an interesting and relevant target in cancer research since its expression is increased in tumor cells. In a recent study, Transferrin covalently attached to silica nanoparticles carrying a hydrophobic drug caused an increase in mortality of the targeted cancer cells compared to cells exposed to nontargeted particles and

free drug (Ferris et al. 2011). What demand further studies though, is the fate of the silica particles in a longer perspective, taken up by tumor cells as well as other cells. A third transport protein, the thyroxin transporting protein Transthyretin, also known to bind toxic components in the blood stream (Hamers et al., 2011), was found to interact with CNO and $SiO_2$. This finding confirms a previous study that pointed out that silica interaction (inhaled) with plasma Transthyretin is contributing to the stabilization of fibroids in rat lungs (Kim et al., 2005). The possible effects of CNO interaction with Transthyretin remains to be investigated.

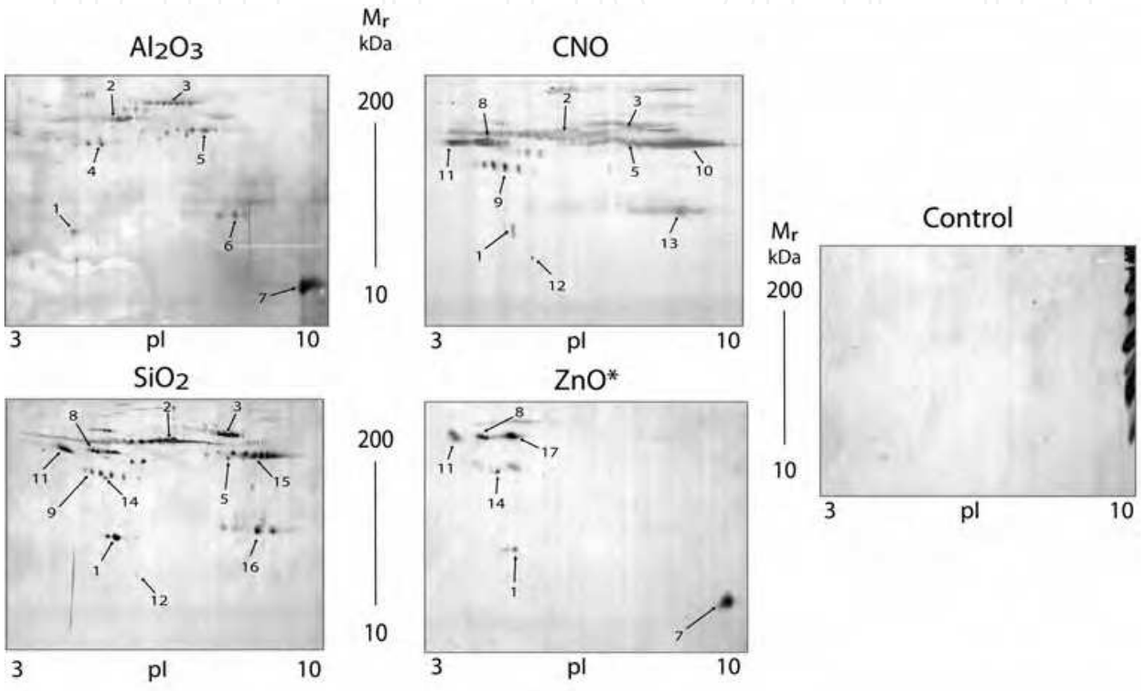


Fig. 5. Plasma protein binding profiles of different nanoparticles.
Four different nanoparticles; $Al_2O_3$, CNO, ZnO (* Aluminium-doped 6%) and $SiO_2$, were mixed with human plasma and isolated through ultracentrifugation. The protein contents were then separated by 2-DE and silver stained. Bound proteins were identified by MS as shown in Table 1.

The inflammatory marker Fibrinogen was found to interact with $SiO_2$, $Al_2O_3$ and CNO but interestingly not with ZnO (Fig 5). Fibrinogen binds foreign substances in the circulation and promotes macrophage activation - a mechanism that may result in retention of particle/protein complexes in the intima with accompanying cardiovascular complications (Shulz et al., 2005). On the other hand, Lysozyme C, a well known anti-bacterial agent, was only found on $Al_2O_3$ and ZnO. Under the present condition, it was unfortunately not determined if the binding to ZnO occurred due to the 6% Al doping of the ZnO. Lysozyme has previously been found to interact with nano-$TiO_2$ particles (Xu et al., 2010). They reported that the coexistence of nano-$TiO_2$ particles and Lysozyme resulted in the transition of Lysozyme conformation from α-helix into β-sheet secondary structure and a substantial inactivation of Lysozyme. Moreover the β-sheets are able to induce the formation of amyloid fibrils, a process which plays a major role in pathology.

| Number in Figure 2 | Protein | Found in Nano particle | Uniprot AccessionNumber | p*I*[a] | Mw[a] (Da) | Matched Peaks[b] | Sequence Coverage (%) | MOWSE Score |
|---|---|---|---|---|---|---|---|---|
| **1** | ApoA-I | $Al_2O_3$, CNO, $SiO_2$, ZNO | P02647 | 5.2 | 24500 | 28 | 74 | 9.65e+10 |
| **2** | Albumin | $Al_2O_3$, CNO, $SiO_2$ | P02768 | 6.0 | 68000 | 30 | 47 | 4.20e+14 |
| **3** | Transferrin | $Al_2O_3$, CNO, $SiO_2$ | Q53H26 | 6.7 | 77000 | 43 | 65 | 1.23e+22 |
| **4** | Fibrinogen γ | $Al_2O_3$ | P02679 | 5.4 | 50000 | 15 | 32 | 1.39e+6 |
| **5** | Fibrinogen β | $Al_2O_3$, CNO | P02675 | 7.0 | 55000 | 17 | 37 | 5.83e+8 |
| **6** | Ig Light chain | $Al_2O_3$ | Q0KKI6 | 7.4 | 30000 | 5 | 32 | 2779 |
| **7** | Lysozyme C | $Al_2O_3$, ZNO | P61626 | 9.4 | 15000 | 7 | 33 | 12888 |
| **8** | α1-AT | CNO, $SiO_2$, ZNO | P01009 | 5.0 | 55000 | 31 | 63 | 5.36e+18 |
| **9** | Haptoglobin | CNO, $SiO_2$ | P00738 | 5.1 | 46000 | 8 | 20 | 2115 |
| **10** | DKFZ | CNO | Q6N096 | 8.3 | 55000 | 14 | 34 | 1.10e+7 |
| **11** | Alpha-2-HS | CNO, $SiO_2$, ZNO | P02765 | 4.8 | 55000 | 6 | 14 | 681 |
| **12** | Transthyretin | CNO, $SiO_2$ | P02766 | 5.4 | 16000 | 7 | 51 | 69267 |
| **13** | Ig KC | CNO | Q6PJF2 | 8.0 | 30000 | 10 | 55 | 409936 |
| **14** | ApoA-IV | $SiO_2$, ZNO | P06727 | 5.1 | 45000 | 10 | 23 | 72729 |
| **15** | Igγ | $SiO_2$ | P01859 | 7.7 | 55000 | 7 | 23 | 79647 |
| **16** | Igγ-1 chain | $SiO_2$ | P01857 | 8.5 | 35000 | 12 | 40 | 3.74e+7 |
| **17** | Amyloid βA4 | ZNO | B4DJT9 | 5.2 | 60000 | 20 | 15 | 53.1 |

Table 1. Identification of nanoparticle bound plasma proteins by peptide mass fingerprinting after 2-DE.
The table shows identified proteins with Uniprot accession number, isoelectric point (pI), molecule weight (Mw), number of peptide masses matched, sequence coverage and MOWSE score. [a] Isoelectric point (pI) and molecular weight (Mw) as estimated on gels. [b] Matched peak masses with a mass error tolerance of 75 ppm.

Furthermore, some antigen binding proteins; IgKC, DKFZ and IgLC, were also found to interact with $Al_2O_3$, CNO and $SiO_2$ but were not detectable on ZnO (Fig 5). Immunoglobulins are able to activate the complement system but they also often represent unspecific binding during protein purification caused by insufficient washing. Our results compared to previous findings indicates that increased hydrodynamic size of nanoparticle agglomerates seems to correlate to increased amounts of immunoglobulins. Overall ZnO was not binding as many proteins as the other particles and may even bind less without being Al-doped but an interesting finding in the ZnO preparation was a protein only described on transcript level and highly similar to the protein Amyloid β A4 precursor. This family of proteins acts as chelators of metal ions such as iron and zinc. They are also able to induce histidine-bridging between beta-amyloid molecules resulting in beta-amyloid-metal aggregates and it has been reported that extracellular zinc-binding increases binding of heparin to Amyloid β A4 (Uniprot 2011).

The protease inhibitor Alpha-1-antitrypsin, was found in the CNO, $SiO_2$ and ZnO preparations but not in $Al_2O_3$ while another antioxidant, Haptoglobin was found only on CNO and $SiO_2$. To our knowledge, the binding of Alpha-1-antitrypsin to the nanoparticles in

this study has not been described previously but an increase of Haptoglobin has been reported in a study investigating acute phase proteins as biomarkers for predicting the exposure and toxicity of nanomaterials (Higashisaka et al., 2011).

At last, the HDL associated Apo A-I, with well known anti-endotoxin activity (Henning et al., 2006) and receptor interaction properties was found in all preparations but was most abundant after $SiO_2$ exposure. Apo A-I may be acting as a scavenger clearing the particles from the blood stream via the scavenger class B-I receptor (SRBI). The SRBI receptor is mainly located on the liver and plays an important role in cholesterol efflux (Verger et al., 2011) but is also present on other cells (Mooberry et al. 2010). Apolipoproteins in general are of interest for the pharmaceutical industry as carriers of nanoparticle bound drugs for brain uptake (Kreuter et al., 2005) since apo E and apo B-100 are taken up by the cells via receptor mediated endocytosis. The hypothesis is that the nano-particle/apolipoprotein complex mimics the natural lipoprotein particle. The identity of Apo A-I was, as the other proteins, confirmed by peptide mass fingerprinting using MALDI TOF MS (Table 1) and one dominating Apo A-I peptide in the MS spectra (Figure 6A) was in addition sequenced by MS/MS (Figure 6B) to further confirm the identity.

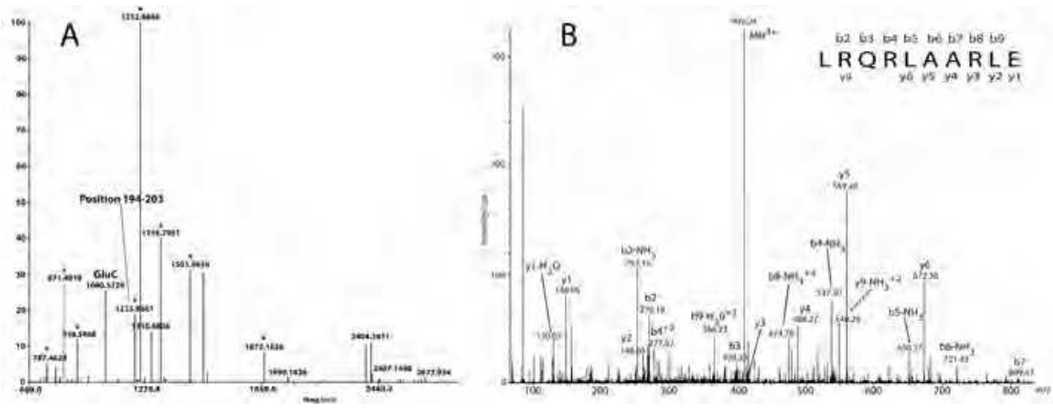


Fig. 6. Identification of nanoparticle bound apoliprotein A-I with mass spectrometry after 2-DE.
A: Peptide mass fingerprint spectrum obtained by MALDI-TOF mass spectrometry after endoproteinase GluC digestion. Asterisks represent peaks corresponding to peptide masses of apo A-I. B: Sequencing of a triply charged peptide (m/z 409.9) corresponding to position 194-203 of apo A-I by collision induced disassociation (CID) in a tandem mass spectrometer. The amino acid sequence with ions corresponding to the different fragments is shown in the upper right corner.

Overall the binding of plasma proteins to nanoparticles, based on previous and our findings, seems to vary with origin, surface properties, size and thereby also diameter of agglomerates. Particle characterization prior to exposure for plasma proteins or cells is therefore extremely important to receive reliable results that are possible to interpret. Interacting proteins under the present conditions are dominated by proteins involved in the immune defense and reverse transport to the liver but notably also proteins mediating brain uptake.

## 4. Methodological considerations and improvements of 2-DE and MALDI-TOF MS

### 4.1 Plasma sample preparations

Sample preparation is an important step that influences the separation of proteins with 2-DE. A common problem in most biological samples is the presence of salt ions. In 2-DE, salt concentrations >10 mM affects the isoelectric focusing step and markedly reduces the effectiveness of the charge separation. There are several easy ways to remove salts, e.g. by precipitation of the proteins or by gelfiltration in small desalting columns. Plasma samples are possible to analyze directly with 2-DE since the high protein concentration allows a simple dilution of the sample to lower the salt concentration. However, as illustrated in figure 7, a desalting step besides the dilution still improves the protein pattern. Another well-known problem with biological fluids is the presence of a few highly abundant proteins that may prevail over the low abundant proteins. In plasma, albumin and immunoglobulin G (IgG) constitutes a very large proportion (about 75%) of the total protein loaded on the gels. This may lead to the proportion of low abundant proteins being below the detection limit. Also, the staining of the abundant proteins may interfere with proteins with similar molecular mass and pI. It is therefore advisable to remove albumin and IgG and there are several commercial removal kits available, usually based on antibodies directed towards albumin and IgG. As shown in figure 7, such sample preparation step removes a large fraction of these proteins and increases the proportion of the other proteins in the sample. However, it is important to realize that this step also introduces unspecific removal of proteins and it is our experience that this unwanted loss of proteins varies considerable between the different available removal kits.

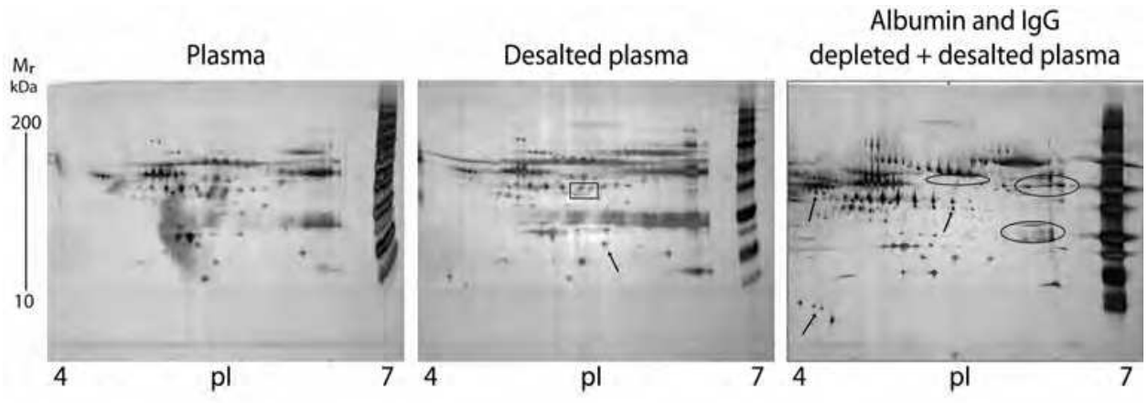


Fig. 7. Preparation of plasma for 2-DE
Untreated plasma (left), desalted plasma (middle) and desalted plasma after removal of albumin and immunoglobulin G (IgG), (right), were separated with 2-DE and silver stained. Arrows indicate protein or protein clusters with increased abundance after treatment compared to untreated plasma. The rectangle indicate an area with improved resolution after desalting. Positions for albumin and IgG chains are indicated with rings.

Plasma contains a wide variety of proteins, many of which are not detectable with 2-DE without further fractionation. In view of the lipid metabolism, important sub-fractions of plasma to study are the lipoproteins. As shown in table 1, one protein that interacts with

nanoparticles is apo A-I, the major constituent of HDL. This implicates the need of more investigations of HDL as a possible target of nanoparticles that may influence the cholesterol metabolism and increase the risk of cardiovascular disease. HDL can be isolated based on density, size or protein content (e.g. apo A-I) using ultracentrifugation, size-exclusion chromatography or immune-affinity chromatography, respectively, each technique with its own merits and drawbacks. Thus, the rather harsh conditions during ultracentrifugation in high salt gradients may remove weakly associated proteins while the rather mild conditions during chromatography may favor unspecific co-purification of proteins with the cholesterol particle. We have previously mapped the protein content of HDL isolated by two-step density gradient ultracentrifugation (Karlsson et al., 2005). In this study we have compared ultracentrifugation and anti-apo A-I affinity chromatography to isolate HDL from the same plasma sample. As shown in figure 8, more proteins were obviously identified in immune-affinity purified HDL. However, some of the proteins must be considered as possible plasma contaminants as they were not, as e.g. the apolipoproteins, enriched in the HDL fraction.

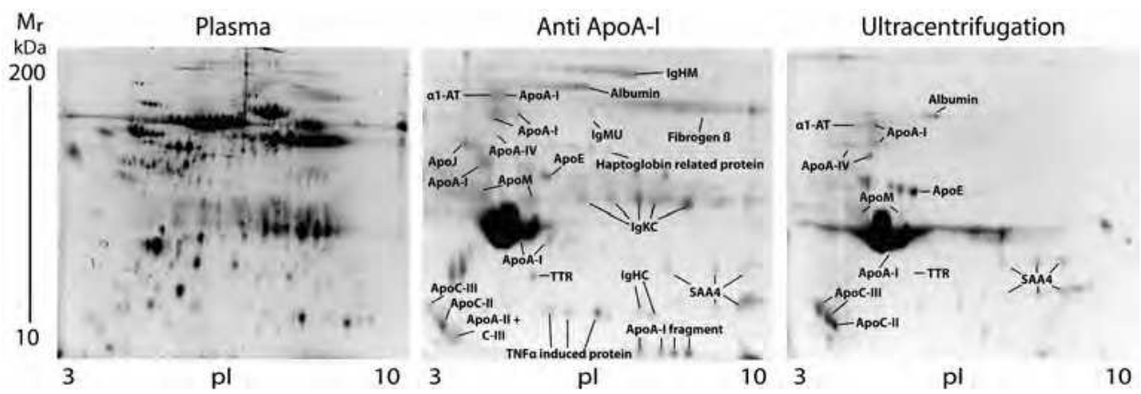


Fig. 8. Subfractionation of plasma with regard to HDL
Plasma (left), HDL purified according to apo A-I with immunoaffinity chromatography (middle) and HDL isolated according to density with ultracentrifugation (right) were separated with 2-DE and silver stained. Proteins were identified with mass spectrometry.

### 4.2 Protein detection

Gel-separated proteins can be visualized by several commonly used staining methods, including dyes (e.g. Coomassie Brilliant Blue and colloidal Coomassie), metals (e.g. silver staining) and fluorescent probes (e.g. Sypro staining and Cy-dyes) (Rabilloud, 2000). The stains interact differently with the proteins and have different limitations with regard to sensitivity, linear range, compatibility with mass spectrometry and type of proteins that stain best. In general, for staining of complex protein samples, silver staining can be considered the most sensitive technique (1-5 ng protein) and Coomassie Brilliant blue the least (50-100 ng) while the sensitivity of colloidal coomassie and the fluorescent dyes are in between. However, it is important to bear in mind that the different stains interact differently with the proteins and therefore one protein may stain very well with one staining method but not with the other (Fig. 9). For example, silver ions react with negatively charged groups and therefore stain glycoproteins containing negative sialic acid very well.

One the contrary, Sypro ruby that binds to proteins through hydrophobic interactions stains hydrophilic glycoproteins quite poorly. Being most sensitive, silver staining is obviously very useful for proteomic approaches. However, the advantage with silver is hampered by its rather low linear range, making it less suitable for quantification than the other staining techniques. For plasma analyses we have therefore adopted a double staining strategy. As illustrated in figure 9, the 2-DE gel is first stained with Sypro Ruby and the proteins are quantified within a high dynamic range. The gel then can be destained and restained by silver to detect additional proteins. As these additional proteins are less abundant their intensities usually are within the limited linear range of the silver staining technique. The proteins may then be selected for MS analyses. As the sample preparation protocol is more time-consuming for silver stained gels than Sypro stained gels it is convenient to pick as many proteins as possible after the first staining step. In this step it is also important to check the optimal destaining time before MS analyses, with plasma samples at least 90 minutes (fig 9). If the samples are not fully destained the signal to noise in the spectra are reduced.

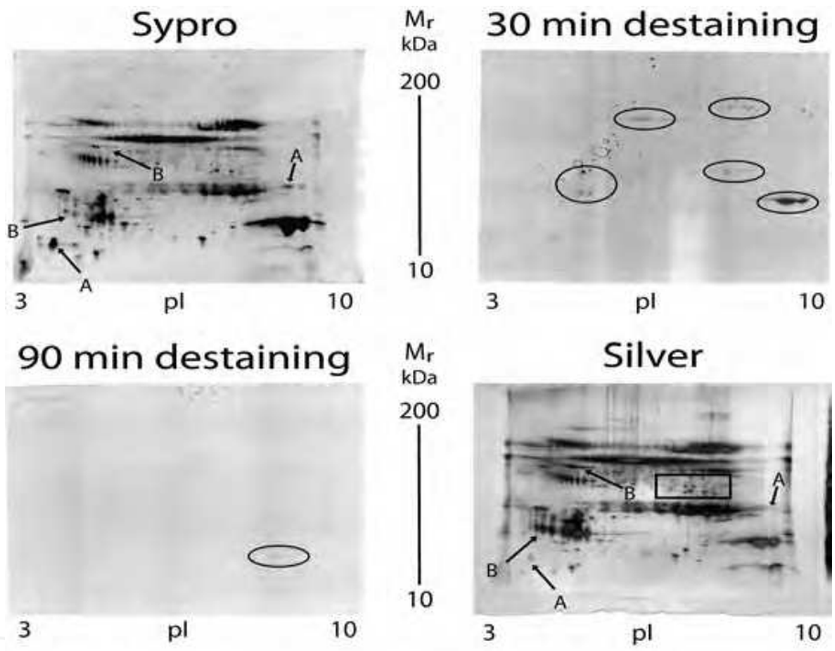


Fig. 9. Double staining of proteins
Plasma proteins were separated with 2-DE and first stained with Sypro Ruby. The gel was then destained with 25 mM ammonium bicarbonate/50 % acetonitrile buffer and the efficiency of the process checked after different time intervals. Finally, the proteins were re-stained with silver. A: Proteins more stained by Sypro compared to silver. B: Glycoproteins more stained by silver. The rectangle shows an area containing additional proteins detected by silver. Residual Sypro staining of proteins after destaining are indicated with rings.

### 4.3 Protein identification with peptide mass fingerprinting using MALDI-TOF MS

Peptide mass fingerprinting with MALDI-TOF MS is an excellent and robust technique for fast identification of plasma proteins after 2-DE (Lahm & Langen, 2000). However, several peptide peaks needs to be detected in the spectra with a high mass accuracy to avoid false

positive results. There are several approaches to consider for improving the data from the analyses, such as digestion protocol, purification of peptides and choice of matrix.

### 4.3.1 Alternative digestion of samples

One of the most widely used ways to digest proteins before MS analyses is by trypsin, which cleaves C-terminally of lysine and arginine (not followed by proline). Although lysine and arginine often are distributed in the protein sequences in a way that provides sufficient number of peptides for identification after trypsin cleavage, this is not always so. Furthermore, it is sometimes necessary to use alternative digestion protocols in order to find specific peptides to e.g. characterize differences between protein isoforms. In these cases alternative enzymes, e.g. Asp-N (cleaves N-terminally of aspartic acid and cystein), Glu-C (C-terminally of glutamic acid) or chemical induced cleavage by CNBr that hydrolyzes C-terminally of methionine, is needed. In this study we used Asp-N as a complement to trypsin when identifying the plasma protein serum amyloid A4 (SAA4). This combined digestion approach generated almost 95 % sequence coverage of the protein (figure 10). SAA4 is a constitutively expressed protein which can be found in HDL as differently charged isoforms (fig 14, Karlsson et al., 2005). One explanation to these isoforms could be a small truncation of SAA4 in which one lysine and one tyrosine is removed C-terminally and thereby making the protein more acidic (Farwig et al., 2005). However, by using Asp-N we were able to detect both the intact C-terminal and the intact N-terminal peptide that were not possible after trypsin digestion, ruling out the presence of truncated SAA4 in our sample (figure 10). Besides the use of Asp-N to study SAA4, we have also used Glu-C to analyze apolipoprotein A-I (figure 6) and CNBr to study serum amyloid A-1/2 isoforms (figure 13).

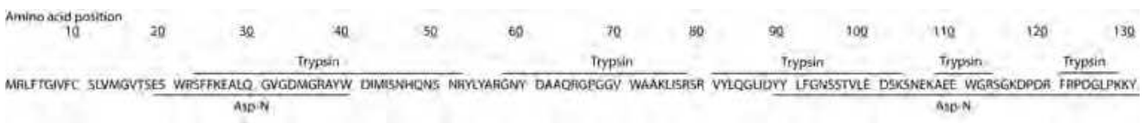


Fig. 10. Alternative digestion to improve sequence coverage of Serum amyloid A4 (SAA4).

Sequence coverage obtained through peptide mass fingerprinting with MALDI-TOF mass spectrometry by the use of trypsin and endoproteinase Asp-N as indicated by the lines. Sequence coverage (without the signal peptide in position 1-18) was 79.5 % with trypsin and 57.1 % with Asp-N. The combined sequence coverage was 93.8%.

### 4.3.2 Peptide sample cleaning

Peptide samples after in-gel digestion can be cleaned by adsorption to C-18 containing pipette tips (ZipTip®). This clean-up procedure done manually is rather time-consuming but is absolutely necessary before electrospray-quadrupole MS. On the other hand, with a MALDI-TOF instrument, being more insensitive to salts and other contaminants, it is not that obvious. To investigate the possible advantage with ziptip cleaning before MALDI-TOF MS we picked 17 sypro stained proteins after 2-DE. The proteins were digested with trypsin and an aliquot of the obtained peptide solution was purified by ZipTip® (50% ACN elution solution according to the protocol recommended by the supplier), mixed with the matrix CHCA and spotted on the MALDI-target plate and another aliquot of the peptide solution was mixed directly with the matrix and spotted on the same plate. All samples were then

analyzed with MALDI-TOF MS with the same settings and with the laser induced collection of spectra in an automatic mode. The spectra were then used for NCBI database search with MS-fit using the same settings for all samples. All 17 proteins were identified with peptide mass fingerprinting in both ziptip cleaned and untreated samples. As shown in Table 2, ziptip cleaning significantly improved the peak intensities, signal to noise ratio and the mass accuracy. This illustrates that removal of salts and other contaminants that will compete with the peptides in the spectra increases the intensities of the peptide peaks and thereby increases the accuracy of the mass determinations and, as a consequence, also increases the reliability of the identifications. On the other hand, the number of peptides and sequence coverage found in ziptip cleaned samples were about the same as in the untreated samples (Table 2). In general, there was a clear tendency that in ziptip cleaned samples more peptides were detected in the lower mass region (<1000 m/z) while fewer peptides were detected in the higher mass region (>2000 m/z). This suggests that the removal of salt ions and low molecular chemicals with subsequent improved signal to noise increases the possibility to detect low molecular mass peptides but that this beneficial effect is counteracted by adsorption of larger peptides to the solid phase of the ziptip. To test this, 10 protein samples were sequential eluted from the ziptip with increasing ACN concentration, up to 90 %. Indeed, this procedure increased the number of peptides found and the sequence coverage increased from 52 +/- 16 % in the untreated samples to 58 +/- 16 in the ziptip cleaned samples ($p<0.05$). The effect varied among the different proteins but was in some samples quite profound, almost 2 times higher sequence coverage. It can be concluded from these experiments that purification of peptide samples with ziptip improves the results with MALDI-TOF MS. However, when it comes to the identification of proteins with peptide mass fingerprinting the beneficial effect of the cleaning procedure is quite limited as the number of peptides found, using the standard protocol, is not increased. Therefore, considering the work-load needed for the ziptip procedure, it is doubtful if it is practical to routinely clean samples with ziptip before MALDI-TOF analyses. However, for selected, low abundant, samples it can most likely make a significant difference for the identification. In these cases, sequential elution of the peptides from the ziptip with increasing acetonitrile concentrations is recommended.

| | Average error (ppm) | Sequence coverage (%) | Number of peptides | Signal/noise ratio | Peak Intensity |
|---|---|---|---|---|---|
| **Without Ziptip (n=17)** | 11.2 +/- 3.6 | 24.9 +/- 12.0 | 8 +/- 4 | 100 +/- 130 | 3500 +/- 2000 |
| **Ziptip (n=17)** | 7.9 +/- 4.4 | 24.1 +/- 11.4 | 8 +/- 3 | 200 +/- 480 | 6300 +/- 4000 |
| **Statistical significance** | 0.01 | No | No | <0.001 | <0.001 |

Table 2. Influence of sample cleanup of in-gel digested proteins on peptide mass fingerprinting data obtained with MALDI-TOF MS.

Proteins were separated by 2-DE and in-gel digested by trypsin. The same peptide samples were then purified by ZipTip, mixed with the matrix and spotted on the MALDI plate or directly mixed with the matrix and spotted on the plate. Statistical interpretations were done by Wilcoxons signed rank sum test.

### 4.3.3 Choice of matrix

To enhance the quality of the MALDI-TOF mass spectra and the number of desorbed peptides there are several matrices that could be considered to use. Different matrix compounds, both acidic and basic, have proved to work in sample preparation for MALDI mass analyzers. The far most commonly used matrix for peptide mass fingerprinting is CHCA, which is recommended for peptides with mass ions below 2500 Da (Beavis et al., 1992). Alternative matrices also used are sinapinic acid, mostly for masses higher than 25 kDa (Lewis et al., 2000) and DHB, originally suggested for glyco- or phosphopepides that are difficult to ionize (Strupat et al., 1991), but later also proven useful for silver stained proteins (Ghafouri et al., 2007). As illustrated in figure 11, CHCA and DHB have very different crystal structures on the target plate. Whereas CHCA usually has a homogeneously distributed spot appearance, making it ideal for automatic laser induced peptide desorption, the DHB crystals are needle shaped and often aggregated into fan-like structures directed from the outside towards the centre of the sample spot. Interestingly, we have found that peptides appear to be enriched in the base of the DHB structures (figure 11), significantly increasing the signal to noise ratio in spectra obtained from these areas. This is illustrated by the identification of transthyretin, one of the proteins that interact with silica nanoparticles and carbon nanotubes (figure 5). With DHB, the improved signal to noise in the spectrum displayed twice the number of peptides than with CHCA (figure 12). This dramatically increased the sequence coverage from 39 % obtained with CHCA to 72 % obtained with DHB. Thus, the use of DHB for low-abundant silver stained proteins from 2-DE is recommended.

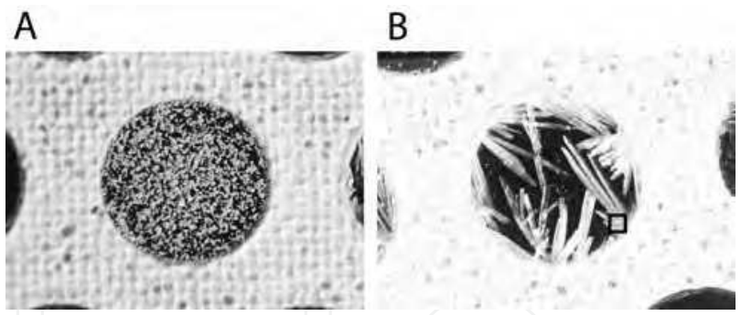


Fig. 11. Crystals of α-cyano-4-hydroxycinnamic acid (CHCA) and 2,5-dihydroxybenzoic acid (DHB).
A; CHCA and B; DHB as matrix on a MALDI plate. The marked area indicates the position of the laser where the best signal to noise was obtained with DHB.

### 4.4 Separation and characterization of isoforms

One of the main challenges for human proteomics is to identify and characterize co- and post-translational modifications to be able to study their relevance and place in systems biology. Most human proteins are expressed as different isoforms often depending on post-translational modifications. Two common modifications in plasma are truncations and glycosylations and here we have used the ability of 2-DE to separate such isoforms based on differences in isoelectric point and molecular mass.

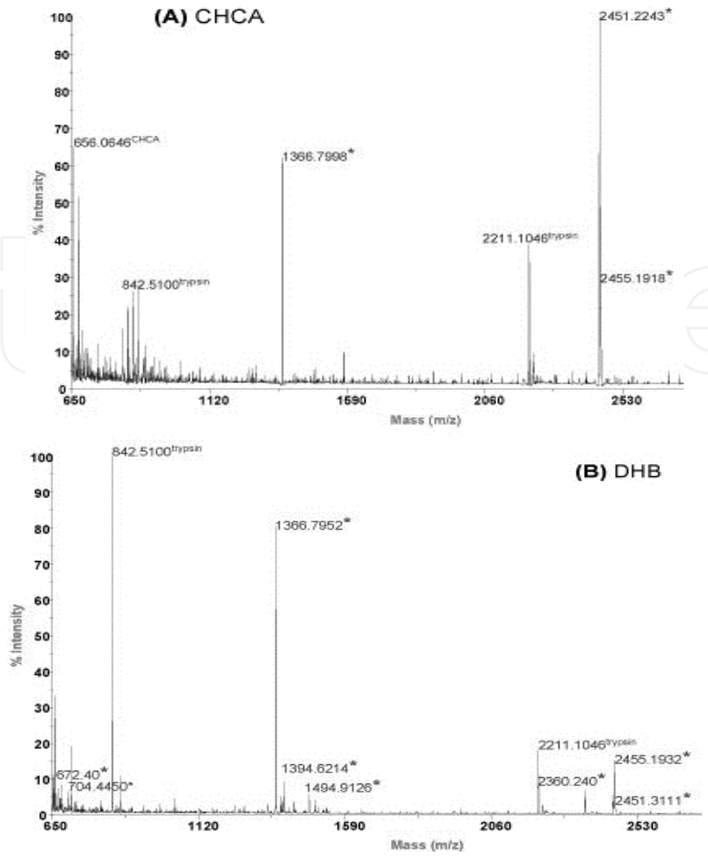


Fig. 12. Comparison of α-cyano-4-hydroxycinnamic acid (CHCA) and 2,5-dihydroxybenzoic acid (DHB) as matrices in MALDI-TOF MS of a silver stained protein.
Transthyretin was identified with sequence coverage of 39 % with CHCA (A) versus 72 % with DHB (B). Peptide peaks marked with an asterisk were matched to the theoretical masses with an accuracy <50 ppm.

Serum amyloid A1 and A2 (SAA1 and SAA2, respectively) are two acute phase proteins, which share more than 95 % sequence identity. Both SAA1 and SAA2 can also be expressed as an alpha- and a beta-form, which are discriminated from the others only in one amino acid position (Strachan et al., 1989). SAA1 and SAA2 are associated to HDL (Karlsson et al., 2005) and are heavily induced by endotoxins (Levels et al., 2011), which is highly relevant in particle toxicology to discriminate between different environmental agents (Karlsson et al. 2011). Based on differences in isoelectric points we were able to separate four isoforms of SAA1/2 in HDL (figure 13A). By peptide mass fingerprinting after trypsin digestion we identified two of the isoforms as SAA1α with pI 5.5 and 6 and two as SAA2α with pI 7 and 8 (figures 13A and 13B). The theoretical pI of SAA1α and SAA2α is 5.9 and 8.3, respectively. Thus, the pI of one of the isoforms of SAA1 and of SAA2 corresponded to the theoretical values while the other two had an acidic shift (pI 6→5.5 in SAA1α and pI 8→7 in SAA2α). N-terminal truncations of SAA1 and SAA2 that would produce such acidic shifts have previously been described (Ducret et al., 1996) and we therefore focused the MS analyses on the N-terminal peptide. As SAA1 and SAA2 contain arginine at the N-terminus we used CNBr, which cleaves before methionines, as an alternative digestion agent to detect the full length N-terminal peptide. These analyses

showed that the more acidic isoforms of SAA1 and SAA2 comprised a mixture of truncations with the loss of one, two or four amino acids N-terminally; des-Arg, des-Arg-Ser and des-Arg-Ser-Phe-Phe, respectively, with the loss of arginine being the main explanation to the acidic shifts (figure 13D). On the other hand, the native peptide was only found in the more basic isoforms of SAA1 and SAA2. In total, four forms of SAA1α and four forms of SAA2α was identified. Interestingly, studies of these small molecular mass variants of SAA1 and SAA2 with SELDI-TOF MS indicates population cluster differences in HDL related to the truncations in response to endotoxin (Levels et al., 2011).

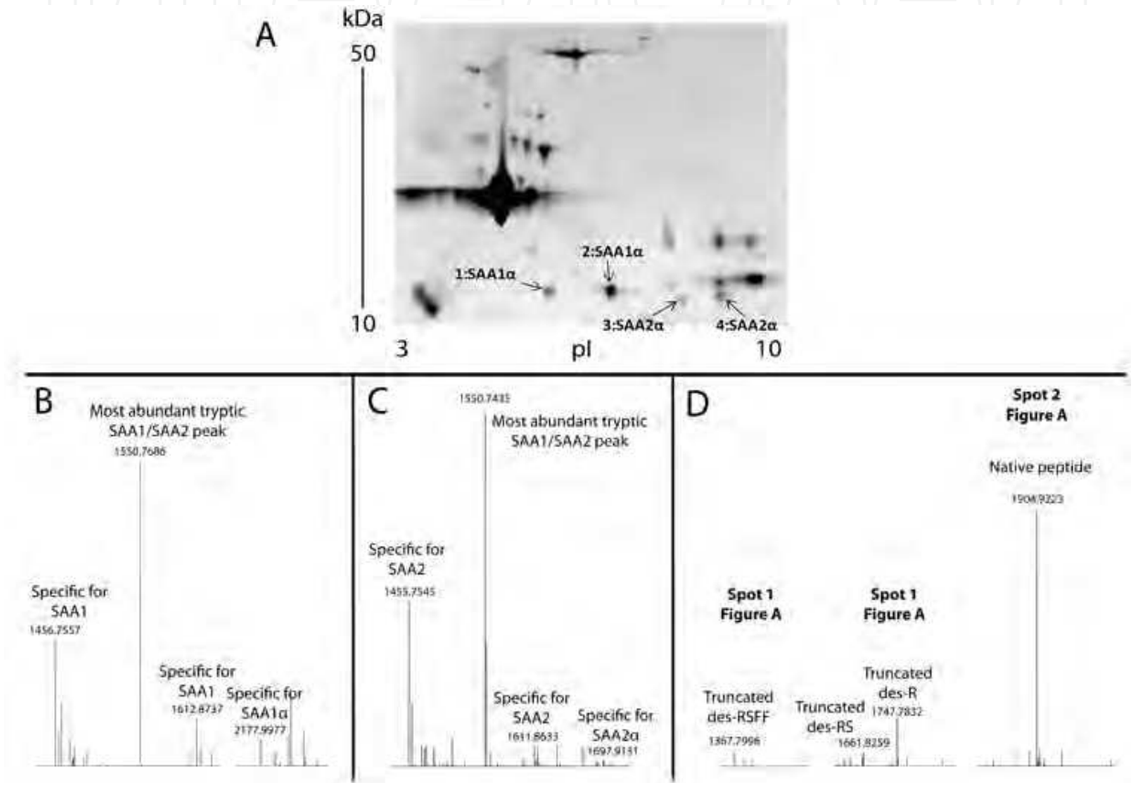


Fig. 13. Identification of serum amyloid A isoforms by 2-DE and MALDI-TOF MS.
A: HDL proteins were separated by 2-DE and stained by Sypro Ruby. Arrows indicate the two isoforms of serum amyloid A1α (SAA1α) and the two isoforms of serum amyloid A2α (SAA2α) identified by peptide mass fingerprinting. B and C: MS spectra after trypsin digestion of SAA1α and SAA2α, respectively, with specific masses indicated. D: MS spectra after CNBr digestion of SAA1α. Masses corresponding peptides from N-terminal truncated variants of the protein (protein spot 1) and the mass corresponding to the N-terminal peptide of the native protein (protein spot 2) are indicated.

2-DE makes it possible to separate proteins based on the degree of glycosylation. Hydrophilic sugars affect the binding of SDS and usually render the proteins an apparent higher molecular mass in the second dimension and the presence of negative sialyl-groups makes the proteins more acidic in the first dimension. We have therefore adapted two simple 2-DE mobility shift assays to demonstrate glycosylation of proteins and applied these to study glycosylated isoforms of plasma proteins in HDL. In the first we use

endoglycosidase PNGase to cleave N-linked oligosaccharides from the protein backbone and the second is based on enzymatic removal of sialic acid with neuraminidase. As shown in figure 14A, SAA4 is usually expressed in HDL as 6 isoforms, three with molecular masses about 18k and three with molecular masses about 11k. After PNGase treatment it was clearly shown that the 18k isoforms are depending on N-linked glycosylation (Fig 14A). Another glycosylated protein in HDL is apo C-III that can be found as three isoforms; one di-sialylated, one mono-sialylated and one minor non-sialylated form (Bruneel et al., 2008). This was demonstrated by treatment with neuraminidase, which induced a mobility shift with the loss of the two sialylated isoforms and a substantial increase of the non-sialyated apo C-III form (figure 14B).

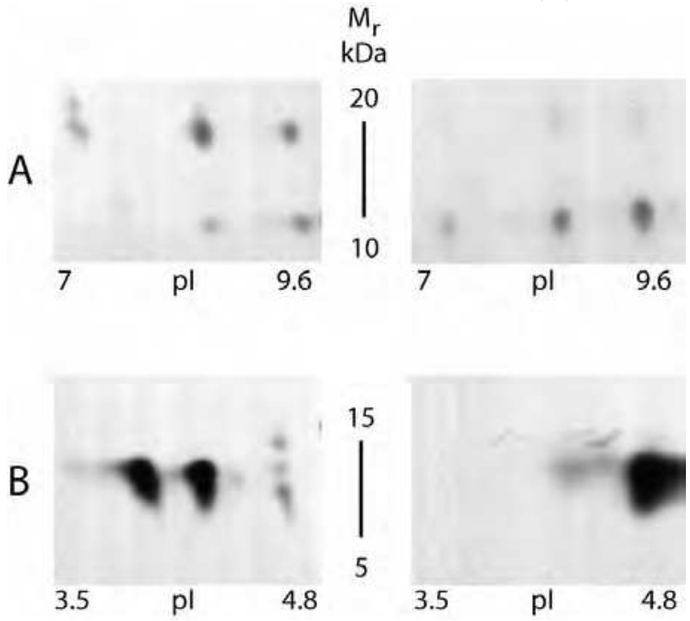


Fig. 14. 2-DE mass and charge mobility shift assays to demonstrate glycosylated protein isoforms.
A: SAA4 analyzed by 2-DE and silver stained. N-linked glycosylated serum amyloid A4 (SAA4) isoforms shown by deglycosylation with PNGase. B: Apo C-III analyzed by 2-DE and Western blots. Sialylated apo C-III isoforms shown by desialylation with neuraminidase.

## 5. Conclusions and future research

Overall the binding of plasma proteins to nanoparticles, based on our findings, seems to vary with origin, surface properties and size of the particles. A large portion of the interacting proteins we identified by 2-DE/MS are proteins involved in the immune defense and reverse cholesterol transport to the liver, but we also identified proteins mediating brain uptake. Most likely these protein patterns of the nanoparticles represent a mixture of particle-protein and protein-protein interactions. Extensive research in this field is therefore needed before conclusions could be drawn regarding potential health effects of nanoparticles and their associated protein "corona". One major difficulty to overcome is how to characterize the particles used in different studies in such a way that comparisons

and generalized conclusions are allowed. Most types of nanoparticles seem to form aggregates, especially so in water suspensions and the "corona" seen might be heavily influenced by the size/diameter of these aggregates rather than by other particle characteristics. Thus, characterization of particles and the aggregates they form prior to exposure of plasma proteins, cells or other biological systems is therefore extremely important. One way of doing that, as we have showed herein, is by DLS. These analyses gives valuable information about the trends in size distribution connected to sample preparation methods and choice of solvent. Sample preparation methods are indeed very important as well as choice of solvent and care should be taken when choosing fitting model and the model-inbuilt parameters. Thus, information obtained from DLS is important for everybody that is doing research on nanoparticles in liquids. The numbers given as product information i.e. the size and size distribution are often relevant for the core-size of the nanocrystals within the material. However the nanoparticles are most often not soluble to that extent. Consequently, nanoparticles obtained in dry state and then dispersed in liquid usually form aggregates as shown in this study.

Given ample attention to the characterization of the NPs used, future studies of the NP–protein complex behavior in different biological systems are needed. Questions that need to be addressed are which properties of the NPs that govern the protein "corona" formed around the NPs in biological fluids and how these complexes interact with endothelial cells, platelets, cells of the immune system etc. One interesting finding in this study is Amyloid β A4, not previously identified in plasma, which was only associated to ZnO particles. This protein may act as a chelator forming metal-amyloid aggregates and needs further attention in toxicological studies.

In summary, the improved 2-DE/MS protocols shown herein underline this proteomic approach as a powerful tool in human nano-particle toxicology. Furthermore, thorough characterisation of the particles studied, e.g. with DLS, is crucial to evaluate the results.

## 6. References

Adiseshaiah, P.; Hall, J. & McNeil, S. E. (2010). Nanomaterial Standards for Efficacy and Toxicity Assessment. *Wiley Interdisciplinary Reviews – Nanomedicine and Nanobiotechnology,* Vol.2, No.1, pp. 99–112, ISSN 1939-0041

Beavis R.; Chaudhary T. & Chait B. (1992). α-Cyano-4-hydroxycinnamic acid as a matrix for matrixassisted laser desorption mass spectrometry. *Organic Mass Spectrometry*, Vol.27, No.2, pp. 156-158

Beck-Speier, I.; Dayal, N.; Karg, E.; Maier, K.; Schumann, G.; Schulz, H.; Semmler, M.; Takenaka, S.; Stettmaier, K.; Bors, W.; Ghio, A.; Samet, J. & Heyder, J. (2005). Oxidative stress and lipid mediators induced in alveolar macrophages by ultrafine particles. *Free Radical Biology and Medicine,* Vol.38, No.8, pp. 1080-1092, ISSN 0891-5849

Bell M. & Davis D. (2001). Reassessment of the lethal London Fog of 1952: Novel Indicators of Acute and Chronic Consequences of Acute Exposure to Air Pollution. *Environmental Health Perspectives,* Vol.109, pp. 389-394, ISSN 0091-6765

Benderly, M.; Boyko, V. & Goldbourt, U. (2009). Apolipoproteins and Long-Term Prognosis in Coronary Heart Disease Patients. *American Heart Journal*, Vol.157, No.1, pp. 103–110, ISSN 1097-6744

Brunauer, S.; Emmett, P. & Teller, J. (1938). Adsorption of Gases in Multimolecular Layers. *Journal of American Chemical Society*, Vol.60, pp.309-319.

Cedervall, T.; Lynch, I.; Lindman, S.; Berggard, T.; Thulin, E.; Nilsson, H.; Dawson, K. & Linse, S. (2007).

Understanding the Nanoparticle-Protein Corona Using Methods to Quantify Exchange Rates and Affinities of Proteins for Nanoparticles. *Proceedings of the National Academy of Sciences of the U.S.A*. Vol.104, No.7, pp. 2050–2055, ISSN 0027-8424

Cherukuri, P.; Gannon, C.; Leeuw, T.; Schmidt, H.; Smalley, R.; Curley, S. & Weisman R. (2006). Mammalian pharmacokinetics of carbon nanotubes using intrinsic near-infrared fluorescence. *Proceedings of the National Academy of Sciences of the U.S.A,* Vol.103, No. 50, pp. 18882-18886, ISSN 0027-8424

Da Silva, E.; Tsushida, T. & Terao, J. (1998). Inhibition of mammalian 15-lipoxygenase-dependent lipid peroxidation in low-density lipoprotein by quercetin and quercetin monoglucosides. *Archives of Biochemistry and Biophysics*, Vol.349, No.2, pp. 313-320, ISSN 0003-9861

Deng, Z.; Mortimer, G.; Schiller, T.; Musumeci, A.; Martin, D. & Minchin R. (2009). Differential plasma protein binding to metal oxide nanoparticles, *Nanotechnology*, Vol.20, No.45, ISSN 1361-6528

Dobrovolskaia, M. & McNeil, S. (2007). Immunological Properties of Engineered Nanomaterials. *Nature Nanotechnolology,* Vol.2, No.8, pp. 469–478, ISSN 1748-3395

Dobrovolskaia, M.; Patri, A.; Zheng, J.; Clogston, J.; Ayub, N.; Aggarwal, P.; Neun, B.; Hall, J. & McNeil, S. (2009). Interaction of Colloidal Gold Nanoparticles with Human Blood: Effects on Particle Size and Analysis of Plasma Protein Binding Profiles. *Nanomedicine,* Vol.5, No.2, pp. 106–117, ISSN 1549-9642

Ducret A.; Bruun C.; Bures E.; Marhaug G.; Husby G. & Aebersold R. (1996). Characterization of human serum amyloid A protein isoforms separated by two-dimensional electrophoresis by liquid chromatography/electrospray ionization tandem mass spectrometry. *Electrophoresis*, Vol.17, No.5, pp. 866-876, ISSN 0173-0835

Dutta, D.; Sundaram, S.; Teeguarden, J.; Riley, B.; Fifield, L.; Jacobs, J.; Addleman, S.; Kaysen, G.; Moudgil, B. & Weber, T. (2007). Adsorbed proteins influence the biological activity and molecular targeting of nanomaterials. *Toxicological Sciences,* Vol.100, No.1, pp. 303-315, ISSN 1096-6080

Elsaesser, A. & Howard, C. (2011). Toxicology of nanoparticles. *Advanced Drug Delivery Reviews*, ISSN 1872-8294

Farwig Z.; McNeal C.; Little D.; Baisden C. & Macfarlane R. (2005). Novel truncated isoforms of constitutive serum amyloid A detected by MALDI mass spectrometry. *Biochemical and Biophysical Research Communications* Vol.332, No.2, pp. 352–356

Ferris, D.; Lu, J.; Gothard, C.; Yanes, R.; Thomas, C.; Olsen, J.; Stoddart, J.; Tamanoi, F. & Zink, J. (2011). Synthesis of biomolecule-modified mesoporous silica nanoparticles for targeted hydrophobic drug delivery to cancer cells. *Small,* Vol.7, No.13, pp. 1816-1826, ISSN 1613-6829

Finsy R. (1994). Particle Sizing by Quasi-elastic light scattering, *Advances in colloid and interface science,* Vol.52, pp. 79-143

Ghafouri, B.; Karlsson, H.; Mortstedt, H.; Lewander, A.; Tagesson, C. & Lindahl, M. (2007). 2,5-Dihydroxybenzoic

acid instead of alpha-cyano-4-hydroxycinnamic acid as matrix in matrix-assisted laser desorption/ionization time-of-flight mass spectrometry for analyses of in-gel digests of silver-stained proteins. *Analytical Biochemistry,* Vol.371, No.1, pp. 121–123, ISSN 0003-2697

Gharahdaghi F.; Weinberg C.; Meagher D.; Imai B. & Mische S. (1999). Mass spectrometric identification of proteins from silver-stained polyacrylamide gel: a method for the removal of silver ions to enhance sensitivity. *Electrophoresis*, Vol.20, No.3, pp. 601-605, ISSN 0173-0835

Görg, A.; Postel, W. & Gunther, S. (1988). The current state of two-dimensional electrophoresis with immobilized pH gradients. *Electrophoresis,* Vol.9, No.9, pp. 531-546, ISSN 0173-0835

Görg ,A.; Obermaier, C.; Boguth, G.; Harder, A.; Scheibe, B.; Wildgruber, R.; and Weiss, W. (2000). The current state of 2-dimensional electrophoresis with immobilized pH gradients. *Electrophoresis.* Vol. 21, No. 12 pp.1037-53

Hackley V. & Clogston J. (2007). Measuring the Size of Nanoparticles in Aqueous Media Using Batch-Mode Dynamic Light Scattering, *NIST-NCL Joint Assay Protocol PCC-1 Version 1.0,* Available from http://ncl.cancer.gov/NCL_Method_NIST-NCL_PCC-1.pdf

Hamers, T.; Kamstra, J.; Cenijn, P.; Pencikova, K.; Palkova, L.; Simeckova, P.; Vondracek, J.; Andersson, P.; Stenberg, M. & Machala, M. (2011) In vitro toxicity profiling of ultrapure non-dioxin-like polychlorinated biphenyl congeners and their relative toxic contribution to PCB mixtures in humans. *Toxicological Sciences,* Vol121, No.1, pp. 88-100, ISSN 1096-0929

Hellstrand, E.; Lynch, I.; Andersson, A.; Drakenberg, T.; Dahlback, B.; Dawson, K.; Linse, S. & Cedervall, T. (2009). Complete High-Density Lipoproteins in Nanoparticle Corona. *FEBS Journal*, Vol.276, No.12, pp. 3372–3381, ISSN 1742-4658

Henning, M.; Garda, H. & Bakas, L. (2006). Biophysical characterization of interaction between apolipoprotein A-I and bacterial lipopolysaccharide. *Cell Biochemistry and Biophysics,* Vol.44, No.3, pp. 490-496, ISSN 1085-9195

Higashisaka, K..; Yoshioka, Y.; Yamashita, K.; Morishita, Y.; Fujimura, M.; Nabeshi, H.; Nagano, K.; Abe, Y.; Kamada, H.; Tsunoda, S.; Yoshikawa, T.; Itoh, N. & Tsutsumi, Y. (2011). Acute phase proteins as biomarkers for predicting the exposure and toxicity of nanomaterials. *Biomaterials,* Vol.32, No.1, pp. 3-9, ISSN 1878-5905

Karlsson H.; Leanderson P.; Tagesson C, & Lindahl M. (2005). Lipoproteomics II: mapping of proteins in high-Density lipoprotein using two-dimensional gel electrophoresis and mass spectrometry. *Proteomics*, Vol.5, No.5, pp. 1431–1445, ISSN 1615-9853

Karlsson, H.; Lindbom, J.; Ghafouri, B.; Lindahl, M.; Tagesson, C.; Gustafsson, M. & Ljungman, A. (2011). Wear particles from studded tires and granite pavement induce pro-inflammatory alterations in human monocyte-derived macrophages: a proteomic study. *Chemical Research in Toxicology,* Vol.24, No.1, pp. 45-53, ISSN 1520-5010

Kim, Y.; Chung, S. & Lee, S. (2005). Roles of plasma proteins in the formation of silicotic nodules in rats. *Toxicology Letters,* Vol.158, No1, pp. 1-9, ISSN 0378-4274

Kreuter, J.; Michaelis, K.; Dries, S. & Langer, K. (2005). The role of apolipoproteins on brain uptake of nanoparticle-bound drugs, *Proceedings of 15th International symposium on Microencapsulation,* Parma, Italy, September 2005

Kreyling, W.; Semmler, M.; Erbe, F.; Mayer, P.; Takenaka, S. & Schulz, H. (2002). Translocation of ultrafine insoluble iridium particles from lung epithelium to extra pulmonary organs is size dependent but very low. *Journal of Toxicology and Environmental Health.* Vol.65, No.20, pp. 1513-1530, ISSN 1528-7394

Kreyling, W.; Semmler-Behnke, M. & Moller, W. (2006). Ultrafine particle-lung interactions: does size matter? *Journal of Aerosol Medicine,* Vol.19, No.1, pp. 74–83, ISSN 0894-2684

Lahm H. & Langen H. (2000). Mass spectrometry: a tool for the identification of proteins separated by gels. *Electrophoresis*, Vol.21, No.11, pp. 2105–2114, ISSN 0173-0835

Leszczynski, J. (2010). Bionanoscience: Nano Meets Bio at the Interface. *Nature Nanotechnology*, Vol.5, No.9, pp. 633–634, ISSN 1748-3395

Levels, J.; Geurts, P.; Karlsson, H.; Maree, R.; Ljunggren, S.; Fornander, L.; Wehenkel, L.; Lindahl, M.; Stroes, E.; Kuivenhoven, J. & Meijers, J. (2011). High-density lipoprotein proteome dynamics in human endotoxemia. *Proteome Science*, Vol.9, No.1, ISSN 1477-5956

Lewis, J.; Wei, J. & Siuzdak G. (2000). Matrix-assisted Laser Desorption/Ionization Mass Spectrometry in Peptide and Protein Analysis. In: *Encyclopedia of Analytical Chemistry*, Meyers, R., pp. 5880–5894, John Wiley & Sons Ltd, ISBN 978-0-471-97670-7, Chichester

Lundqvist, M.; Stigler, J.; Elia, G.; Lynch, I.; Cedervall, T. & Dawson, K. (2008). Nanoparticle Size and Surface Properties Determine the Protein Corona with Possible Implications for Biological Impacts. *Proceedings of the National Academy of Sciences of the U.S.A,* Vol.105, No.38, pp. 14265–14270, ISSN 1091-6490

Lynch, I.; Cedervall, T.; Lundqvist, M.; Cabaleiro-Lago, C.; Linse, S. & Dawson, K. (2007). The Nanoparticle-Protein Complexas a Biological Entity; a Complex Fluids and Surface Science Challenge for the 21st Century. *Advances in Colloid and Interface Science*, Vol.134-135, ISSN 0001-8686

McAuliffe, M. & Perry, M. (2007). Are nanoparticles potential male reproductive toxicants? A literature review. *Nanotoxicology.* Vol.1, No.3, pp. 204-210

Mooberry, L.; Nair, M.; Paranjape, S.; Mc Conathy, W. & Lacko, A. (2010). Receptor mediated uptake of pacilitaxel from synthetic high density lipoprotein nancarrier. *Journal of drug targeting,* Vol.18, No.1, pp. 53-58, ISSN 1029-2330

Mühlfeld, C.; Rothen-Rutishauser, B.; Blank, F.; Vanhecke, D.; Ochs, M. & Gehr, P. (2008). Interactions of nanoparticles with pulmonary structures and cellular responses. *American Journal of Physiology - Lung Cellular and Molecular Physiology.*Vol. 294, No.5, pp. L817-L829, ISSN 1040-0605

O'Farrell, P.H. (1975). High-resolution two-dimensional electrophoresis of proteins. *J Biol Chem.* 250, pp. 4007–4021

Rabilloud, T. (2000. Detecting proteins separated by 2-D gel electrophoresis. *Analytical Chemistry.* Vol.72, No.1, pp. 48A-55A, ISSN 0003-2700

Rothen-Rutishauser, B.; Muhlfeld, C.; Blank, F.; Musso, C. & Gehr, P. (2007). Translocation of particles and inflammatory responses after exposure to fine particles and nanoparticles in an epithelial airway model. *Particle and Fibre Toxicology*, Vol.4, No.9, ISSN 1743-8977

Sattler, W.; Mohr, D. & Stocker, R. (1994). Rapid isolation of lipoproteins and assessment of their peroxidation by high-performance liquid chromatography postcolumn chemiluminescence. *Methods in Enzymology,* Vol.233, pp. 469-489, ISSN 0076-6879

Schulz, H.; Harder, V.; Ibald-Mulli, A.; Khandoga, A.; Koenig, W.; Krombach, F.; Radykewicz, R.; Stampfl, A.; Thorand, B. & Peters, A. (2005). Cardiovascular effects of fine and ultrafine particles. *Journal of Aerosol Medicine,* Vol.18, No.1, pp. 1-22, ISSN 0894-2684

Shevchenko, A.; Wilm, M.; Vorm, O. & Mann, M. (1996). Mass spectrometric sequencing of proteins silver-stained polyacrylamide gels. *Analytical Chemistry,* Vol.68, No.5, pp. 850-858, ISSN 0003-2700

Shevchenko, A.; Chernushevich, I.; Shevchenko, A.; Wilm, M. & Mann, M. (2002). De novo sequencing of peptides recovered from in-gel digested proteins by nanoelectrospray tandem mass spectrometry. *Molecular Biotechnology,* Vol.20, **No.1,** pp. 107-118, ISSN 1073-6085

Sorensen, C. (2008). Scattering and Absorption of Light by Particles and Aggregates, *Handbook of Surface and Colloid Chemistry Third Edition,* Birdi K., CRC Press, ISBN 978-0-8493-7327-5, Boca Raton, Florida, US

Stern, S. & McNeil, S. (2008). Nanotechnology safety concerns revisited. *Toxicological Sciences,* Vol.101, No.1, pp. 4-21, ISSN 1096-6080

Strachan A.; Brandt W.; Woo P.; van der Westhuyzen D.; Coetzee G. & de Beer M. (1989). Human serum amyloid A protein. The assignment of the six major isoforms to three published gene sequences and evidence for two genetic loci. *Journal of Biological Chemistry,* Vol.264, No.31, pp. 18368-18373, ISSN 0021-9258

Strupat K.;,Karas M. & Hillenkamp F. (1991). 2,5-Dihydroxybenzoic acid: a new matrix for laser desorption—ionization mass spectrometry. *International Journal of Mass Spectrometry and Ion Processes*, Vol.111, pp. 86-102, ISSN 0168-1176

Uniprot. (2011). Amyloid beta A4 protein, 20th October 2011, Available from http://www.uniprot.org/uniprot/P05067

Vergeer, M.; Korporaal, S.; Franssen, R.; Meurs, I.; Out, R.; Hovingh, G.; Hoekstra, M.; Sierts, J.; Dallinga-Thie, G.; Motazacker, M.; Holleboom, A.; Van Berkel, T.; Kastelein, J.; Van Eck, M. & Kuivenhoven, J. (2011). Genetic variant of the scavenger receptor class B-I in humans. *The New England Journal of Medicine*, Vol.364, No.2, pp. 136-45, ISSN 1533-4406

Walczyk, D.; Bombelli, F.; Monopoli, M.; Lynch, I. & Dawson, K. (2010). What the Cell "Sees" in Bionanoscience. *Journal of the American Chemical Society*, Vol.132, No.16, pp. 5761–5768, ISSN 1520-5126

Wick, P.; Malek, A.; Manser, P.; Meili, D.; Maeder-Althaus, X.; Diener, L.; Diener, P-A.; Zisch, A.; Krug, H.F. & von Mandach, U. (2010). Barrier Capacity of Human Placenta for Nanosized Materials. *Environmental Health Perspectives.* Vol.118, No.3, pp. 432-436, ISSN 1552-9924

Wu, W. & Jiang, X. (2011). A practical strategy for constructing nanodrugs using carbon nanotubes as carriers. *Methods in Molecular Biology,* Vol.751, pp. 565-582, ISSN 1940-6029

Xu, Z.; Liu, X.; Ma, Y. & Gao, H. (2010). Interaction of nano-TiO2 with lysozyme: insights into the enzyme toxicity of nanosized particles. *Environmental Science and Pollutional Research International,* Vol.17, No.3, pp. 798-806, ISSN 1614-7499

Zensi, A.; Begley, D.; Pontikis, C.; Legros, C.; Mihoreanu, L.; Buchel, C. & Kreuter, J. (2010). Human Serum Albumin Nanoparticles Modified with Apolipoprotein a-I Cross the Blood-Brain Barrier and Enter the Rodent Brain. *Journal of Drug Targeting*, Vol.18, No.10, pp. 842–848, ISSN 1029-2330

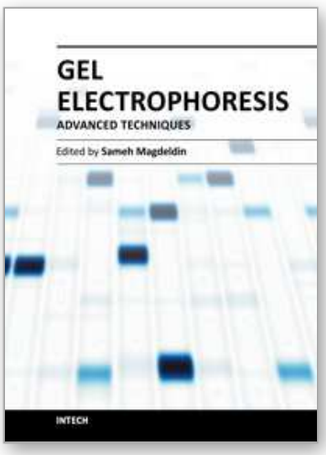


**Gel Electrophoresis - Advanced Techniques**

Edited by Dr. Sameh Magdeldin

ISBN 978-953-51-0457-5
Hard cover, 500 pages
**Publisher** InTech
**Published online** 04, April, 2012
**Published in print edition** April, 2012

As a basic concept, gel electrophoresis is a biotechnology technique in which macromolecules such as DNA, RNA or protein are fractionated according to their physical properties such as molecular weight or charge. These molecules are forced through a porous gel matrix under electric field enabling uncounted applications and uses. Delivered between your hands, a second book of this Gel electrophoresis series (Gel Electrophoresis- Advanced Techniques) covers a part, but not all, applications of this versatile technique in both medical and life science fields. We try to keep the contents of the book crisp and comprehensive, and hope that it will receive overwhelming interest and deliver benefits and valuable information to the readers.

**How to reference**

In order to correctly reference this scholarly work, feel free to copy and paste the following:

Helen Karlsson, Stefan Ljunggren, Maria Ahrén, Bijar Ghafouri, Kajsa Uvdal, Mats Lindahl and Anders Ljungman (2012). Two-Dimensional Gel Electrophoresis and Mass Spectrometry in Studies of Nanoparticle-Protein Interactions, Gel Electrophoresis - Advanced Techniques, Dr. Sameh Magdeldin (Ed.), ISBN: 978-953-51-0457-5, InTech, Available from: http://www.intechopen.com/books/gel-electrophoresis-advanced-techniques/two-dimensional-gel-electrophoresis-and-mass-spectrometry-in-studies-of-nanoparticle-protein-interac

INTECH
open science | open minds

**InTech Europe**
University Campus STeP Ri
Slavka Krautzeka 83/A
51000 Rijeka, Croatia
Phone: +385 (51) 770 447
Fax: +385 (51) 686 166
www.intechopen.com

**InTech China**
Unit 405, Office Block, Hotel Equatorial Shanghai
No.65, Yan An Road (West), Shanghai, 200040, China
中国上海市延安西路65号上海国际贵都大饭店办公楼405单元
Phone: +86-21-62489820
Fax: +86-21-62489821

IntechOpen